(In)stability of ligands at the surface of inorganic nanoparticles: a forgotten question in nanomedicine?

*Marine Le Goas[a], Justine Saber[a], Sara González Bolívar[a], Jean-Michel Rabanel[a], Jean-Marc Awogni[a], Daria C. Boffito[b], Xavier Banquy[a]**

a. Faculty of Pharmacy, Université de Montréal, Montréal, Québec H3C 3J7, Canada
b. Department of Chemical Engineering, Polytechnique Montréal, Montréal, Québec H3C 3A7, Canada

*Corresponding author: xavier.banquy@umontreal.ca

Abstract

Multiple inorganic nanoparticles (NPs) are currently being developed for nanomedicine. Various core materials and shapes are explored, but they all display a common hybrid structure, with organic ligands on their surface. These ligands play a key role in the NP colloidal stability and surface properties, and therefore strongly impact the biological fate of the NPs. However, ligands may be subject to reorganization, degradation, desorption, and exchange, both during their shelf-life and upon exposure to a biological environment. The question of ligand (in)stability at the surface of inorganic NPs has been little addressed in the literature. The goal of this review is to provide a portrait of this critical phenomenon. We identify and review here the different mechanisms likely to promote ligand instability and discuss the resulting biological fate of ligands. This review is aimed to provide a better understanding of these phenomena and to help researchers to design NP-based medicines with better clinical efficacy and translation ability.

Keywords: nanoparticles; nanomedicine; nano-bio interactions; stability; ligand stability; ligand exchange

1. Introduction

Among the great variety of nanoparticles (NPs) studied for biomedical applications, inorganic NPs have attracted much interest. They not only provide a platform for drug delivery, but they also display promising intrinsic properties as therapeutic and imaging agents. Gold NPs (AuNPs) have, for instance, demonstrated their efficacy for photothermal treatment and radiosensitization,[1,2] while iron oxide NPs (IONPs) have been used for magnetic hyperthermia or as MRI contrast agents.[3] The vast majority of inorganic NPs exhibit a hybrid structure composed of an inorganic core coated with organic ligands whose primary function is to ensure colloidal stability and, in some instances, to provide targeting properties.[4,5] Preventing aggregation is indeed key for nanomedicines, as it can strongly impact their biological behavior and even generate some toxicity in vivo.[6–8] Yet, colloidal stability and core degradation are usually the only parameters considered in stability studies of inorganic NPs, and little is known about the fate of the surface coating in biological environments. As we will see, the performance of nanomedicines is however partly determined by their surface ligands.

Firstly, surface chemistry affects the overall stability of the NP. As already mentioned, the NP colloidal stability greatly depends not only on the presence of surface ligands but also on their nature and properties. Multiple studies have shown how the aggregation of various inorganic NPs could be either promoted or prevented by modifying their surface chemistry.[9–11] For instance, multivalent ligands have been shown to provide improved colloidal stability compared to monovalent ones.[12,13] Surface ligands also play a protective role against the surrounding medium and therefore affect the degradation of the inorganic core.[14–16] Secondly, surface chemistry governs the interactions of NPs with the biological environment. The chemical structure, charge, hydrophobic/hydrophilic nature, conformation, organization, and grafting density of the surface ligands have indeed been shown to impact numerous biological phenomena such as NP interaction with proteins and formation of the protein corona[17–19], NP cellular uptake,[20–23] NP cytotoxicity,[24] NP diffusion in biological matrices,[25,26] NP biodistribution,[27,28] and NP clearance.[29–31] Lastly, ligands are frequently used to add targeting moieties,[32] drugs,[33] or fluorescent dyes to the NPs. The moieties can either be used directly as ligands[34,35] or conjugated onto primary surface coatings.[36–38]

As a result, the stability of surface ligands is essential to maintain the properties and efficacy of inorganic NPs. However, *in vivo*, NPs encounter complex environments with challenging

conditions (high ionic strength, high concentrations of biomolecules, acidic pH, etc.) which may cause partial to complete degradation of the ligands or their dissociation from the core. Inorganic NPs are also frequently used in combination with external stimuli, such as radiations or magnetic fields, that can trigger new mechanisms of ligand instability.

Despite the key role of ligands in NP performance, the question of their stability has not been thoroughly investigated and little literature has been published on the subject. The first and main reason is the technological challenge that these studies represent. Monitoring the fate of NPs *in situ*, in biological media or *in vivo*, remains difficult due to the complexity and dynamic characteristics of biological environments, which are not compatible with most recent characterization techniques. The evolution of NP surface chemistry is even more challenging to characterize, considering its organic nature and smaller scale. Instead of *in situ* analyses, one alternative strategy relies on separating the NPs from the biological medium prior to any characterization. This may however alter the biointerface between the particle, the ligands, and the medium. Such an approach is known for instance to affect the protein corona adsorbed at the surface of NPs.[39–41] Furthermore, NP surface characterization remains challenging, even outside of biological media, due to a lack of suitable techniques.[42,43] One additional difficulty lies in the distinction between intact, degraded, and dissociated systems, and their individual quantification. Again, separation techniques may be used, with the same risk of alteration. Multiple labeling strategies have also proven to be powerful to monitor the fate of both ligands and core,[44,45] even though labeling may modify the NP properties.

One second reason for such a lack of literature might be cultural: the nanomedicine community has not questioned ligand stability, originally considering nano-objects as homogeneous entities, even in biological environments or under external stimuli. The possible individual degradation of both components of the NPs (inorganic core and organic coating) has only been recently pointed out,[46,47] thus highlighting the dynamic nature of surface ligands.

We review here the current literature regarding the stability of ligands at the surface of inorganic NPs. The role and nature of the ligands are first briefly described, then the mechanisms of ligand instability that have been reported so far are presented. Finally, the intracellular and *in vivo* ligand biological fates are discussed in light of the currently identified degradation mechanisms.

For our review of the literature, we have looked primarily for studies focusing on ligands anchored on nanoparticulate systems. When scientific reports were scarce, we occasionally

considered results obtained on planar surfaces, as some mechanisms are similar. Yet, the high curvature of NPs and the geometrical defects resulting from it (edges and vertexes) may impact the packing density, the ordering, and the binding affinity of ligands,[48] which can in turn affect ligand reactivity and stability. Although this review focuses on ligand stability in the context of nanomedicine, we have also included studies from other fields of research to bring new, and hopefully broader, perspectives on ligand stability issues.

2. Nature, role, and characterization of organic ligands on inorganic NPs

Several types of inorganic NPs are currently studied in nanomedicine: metallic NPs (gold, silver, and platinum), magnetic IONPs, semiconductor quantum dots (QDs), and silica NPs, for the main ones. As the strength of ligand binding is critical for colloidal stability, the nature of the anchoring groups is chosen according to the chemical composition of the core.[4] Thiols, for instance, have a strong binding affinity for metal NPs, whereas carboxyl and hydroxyl groups are much used with iron oxide surfaces. Direct physisorption has been used for polymers, proteins, and oligonucleotides through electrostatic or hydrophobic interactions, while metal-thiol and metal-amine bonds are considered quasi-covalent and therefore often used to functionalize NP surfaces.[4]

Besides colloidal stability, the use of ligands allows fine-tuning of NP surface properties, and accordingly of their biological behavior. A wide variety of ligands have been designed and tested: small molecules such as citrate or phosphine derivatives, surfactants such as cetyltrimethylammonium bromide (CTAB), polymers, and biomolecules of various sizes, from glucose and glutathione to peptides, DNA, and proteins.[4,49] Poly(ethylene glycol) (PEG) is among the most frequently used ligands in nanomedicine, due to its capacity to bring stealth properties, biocompatibility, and extended blood circulation time to the NPs.[50] The choice of ligands during the synthesis can also result from the need for a specific core morphology.[5] The ligand binding energy can indeed impact the size of the resulting NPs, while some ligands such as CTAB may act as shape-directing agents. The ligands used during the synthesis of the NP core can also be exchanged *a posteriori*, to fine-tune the surface properties.[51] Such ligand exchange process is discussed in detail in the next section.

As already mentioned, apart from the composition of the ligands, their density, organization, and conformation can also greatly impact the NP behavior. As a result, protocols have been developed to modulate ligand density[52,53] or arrangement at the NP surface.[54,55] For more

details about the role of ligands in the synthesis and applications of inorganic NPs, we refer the reader to the review by Heuer-Jungemann *et al.*[4]

Despite the key role of ligands, their characterization remains challenging, as highlighted by previous reviews.[42,43] In Table 1, we give an overview of the techniques that have been used to characterize ligands, and thus their stability. The type of information obtained and the advantages and limitations of each technique are provided, as well as the compatibility with *in situ* measurements in biological environments. Representative references are indicated for all techniques.

Table 1. Techniques commonly used to characterize ligand stability.

Technique	Type of information	Advantages	Limitations	Compatible with *in situ* measurements in biological environments	References
Techniques to characterize ligands					
Raman spectroscopy / SERS	Nature of the NP-ligand chemical bond and chemical structure of the ligands	High sensitivity (SERS)	Low sensitivity (Raman) Degradation issues under the beam Short-range enhancement (few nm) (SERS)	X	[59,110,149,154,185,186,195]
NMR	Chemical structure of the ligands	Easy to use and accessible	Requires large sample amount Low sensitivity Requires non paramagnetic materials		[48,56,87,143,148,216]
XPS	Nature of the NP-ligand chemical bond and chemical structure of the ligands	Semi-quantitative	Tedious sample preparation Dry state, under vacuum Probes only a few nm deep Limited availability		[148,155,163]
IR/ FTIR	Chemical structure of the ligands	Easy to use and accessible High sensitivity	Uniformity and dilution of samples to avoid saturation	X	[48,148,163,233,243,253]
LDI-MS	Chemical structure and composition of the ligands	Semi-quantitative	Destructive Limited availability	X	[217,234]
MALDI-TOF-MS	Ligand composition and morphology	High sensitivity High accuracy	Destructive High cost Limited availability	X	[156]
SEC / Gel electrophoresis	Size of ligands	Separation according to the size	Requires desorption from the NP surface		[89,216]
Techniques to monitor ligand presence at the NP surface					
Fluorescence labeling	Detection of ligand instability via modifications of the fluorescence intensity or via the colocalization with the core	Accessible High sensitivity	Requires fluorescent labeling Requires purification from unbound ligands (without colocalization)	X	[45,89,111,245,247]
Fluorescence quenching / FRET	Detection of ligand instability via the recovery of the fluorescence intensity	Detection in very close distances Semi-quantitative	Requires fluorescent labeling (and quencher labeling in some cases)	X	[113,132,207,240,246,248,254]

FLIM	Detection of ligand instability via modifications of the core fluorescence lifetime	High sensitivity Independent on the concentration (compared to intensity-based measurements)	Requires a fluorescent core	X	[135,249]
SPR / UV-vis spectroscopy	Detection of ligand instability via modifications of the core signal	Fast analysis Easy to use and accessible	Requires a photoluminescent or plasmonic core	X	[61,63,154,185,188,189]
Radiolabeling	Detection of ligand instability via the colocalization with the core	High sensitivity	Handling of radioactive materials High cost	X	[44,45,134,239]
Size measurement techniques (such as DLS)	Detection of ligand instability via modifications of the NP size	Easy to use Accessible	Low sensitivity Very sensitive to aggregation		[106]
TGA	Ligand quantity, detection of ligand reorganization	Quantitative Easy to use and accessible	Requires large sample amount Low sensitivity for large NPs Requires purification from unbound ligands		[110,142]
SANS / SAXS	Detection of ligand instability via modifications of the NP size and structure, quantification of ligands	Can be quantitative (depending on the model) Versatile thanks to contrast matching (in SANS)	Model-dependent Complex analysis Limited availability Degradation issues under the beam	X	[216]
Colorimetric assays	Ligand quantity	Fast analysis Easy to use	Possible interferences from the NP Low sensitivity		[110,174]

Abbreviations: SERS: surface-enhanced Raman spectroscopy; NMR: nuclear magnetic resonance spectroscopy; XPS: X-ray photoelectron spectroscopy; IR: infrared spectroscopy; FTIR: Fourier-transform infrared spectroscopy; LDI-MS: laser desorption/ionization mass spectrometry; MALDI-TOF-MS: matrix-assisted laser desorption/ionization time-of-flight mass spectrometry; SEC: size exclusion chromatography; FRET: Förster resonance energy transfer; FLIM: fluorescence lifetime imaging microscopy SPR: surface plasmon resonance; DLS: dynamic light scattering; TGA: thermogravimetry analysis; SAXS/SANS: small-angle X-ray/neutron scattering.

3. Mechanisms of ligand instability

When considering the stability of NPs, a distinction should be made between stability issues occurring during storage and upon exposure to a biological environment. Storage stability of NPs, either in their dry form or in suspension, is one key consideration for clinical translation and has been largely overlooked in the literature. Yet, degradation can readily happen through spontaneous mechanisms and hence affect the biological performance of the particles. Surface coating is no exception, as shown by Carregal-Romero *et al.*[56] Upon exposure to biological media, many transformation mechanisms of the NP can occur, reflecting the complexity of the interactions between the NP and its biological environment. In this section, we describe the different mechanisms that affect ligand stability in these two contexts. These mechanisms are schematically represented in **Figure 1**.

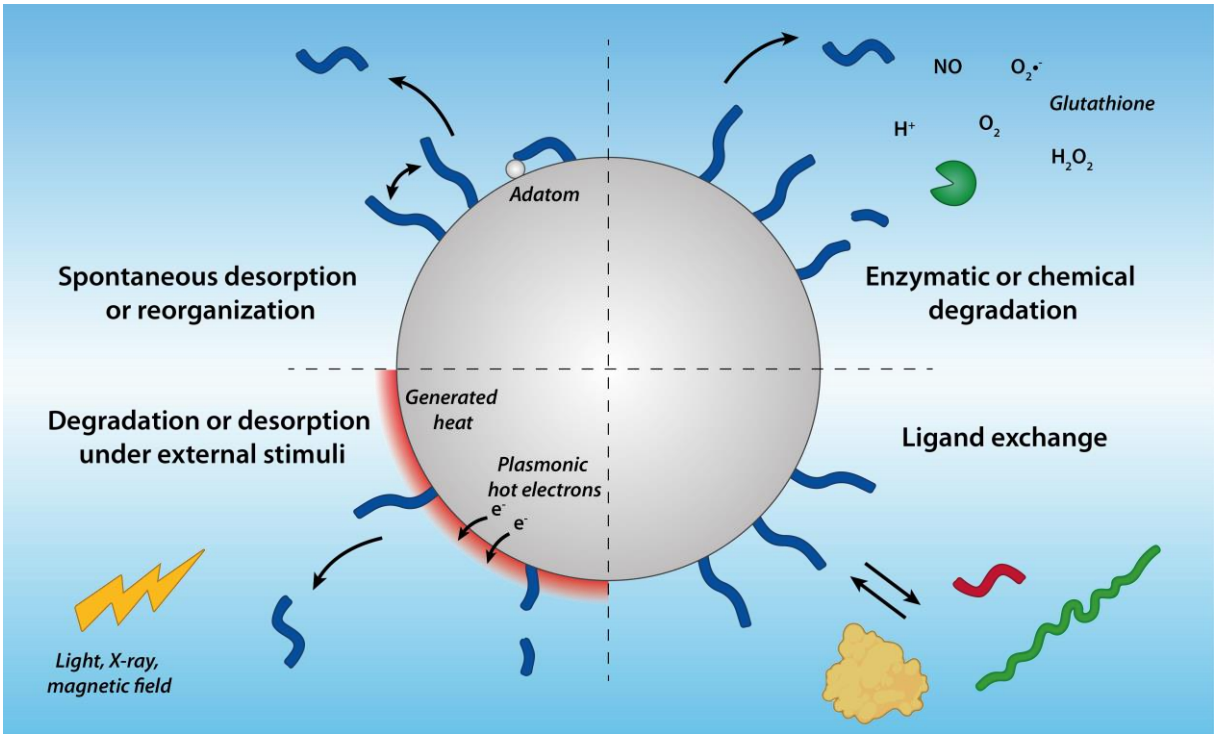

Figure 1. Schematic representation of the different mechanisms that can affect ligand stability. Figure created with the help of Biorender.com.

3.1. Spontaneous reorganization and desorption

One reported mechanism is the spontaneous reorganization of surface ligands over time. This phenomenon was first hypothesized from indirect observations. For instance, Chechik has revealed a reduction in the exchange rate of ligands with disulfides on aged thiolate-protected AuNPs.[57] The same author later further analyzed the kinetics of two reactions: AuNP ligand exchange with disulfides, and cyanine-induced AuNP decomposition. In both cases, reduced reactivity was observed after AuNP aging in solution (up to almost 200 hours).[58] The authors hypothesized that this was due to a surface reorganization process: over time, the defect sites involved in the reactions become better coordinated to other gold atoms and as a consequence, the thiolates attached to these sites become less labile.

Recently, more direct demonstrations of this spontaneous reorganization were obtained. Grys *et al.* used surface-enhanced Raman spectroscopy (SERS) to follow Au-citrate coordination in both fresh and 35-day aged citrate-coated AuNPs.[59] Aging was found to involve the displacement atop the AuNP facets of gold adatoms which facilitated the binding of two carboxylate functions of citrate, instead of one as observed for fresh AuNPs (**Figure 2A**). This phenomenon can improve the stability of the ligands and consequently decrease their reactivity, as previously reported by Chechik *et al.*[57,58] Interestingly, adatoms could be removed using etching and subsequent boiling of the AuNPs, thus bringing the surface back to its original coordination state.

In another recent study, Horáček *et al.* used DNA-functionalized gold nanorods (AuNRs) and DNA-hybridization kinetics to analyze single-molecule binding events and reveal the number of docking strands per particle.[60] When testing two different functionalization methods, a strong heterogeneity in ligand density was observed at short functionalization times, but homogeneity increased when extending the incubation time over several hours to days (**Figure 2B**). Similar behavior was reported for particles aged in buffer (*i.e.*, with negligible residual free ligands), therefore excluding ligand exchange as a possible explanation. The authors concluded from their experiments that the increase in homogeneity upon aging mainly originates from ligand reorganization, which may involve changes in ligand accessibility, desorption of non-specifically bound ligands, or diffusion of interfacial gold atoms.

Interestingly, spontaneous desorption of ligands from the surface of cadmium selenide (CdSe) nanocrystals was observed upon protonation of thiolate anchoring groups at low pH (between

2 and 7 depending on the NP size).[61] Ligand loss was also reported on diluted and aged suspensions of similar objects.[62] Similarly, alkylthiol-stabilized AuNPs exhibited ligand loss under a variety of storage conditions, demonstrating the importance and predominance of the phenomenon.[63] Even though the two last studies show the key role of aging on ligand stability, the mechanisms underlying the surface transformations experienced by the NPs were not explored.

These studies demonstrate that surface ligands should be considered dynamic rather than unalterable elements. Their coordination state, conformation, and location on the NP surface may evolve over time, even leading to desorption in some cases. Other mechanisms may however trigger the spontaneous desorption of ligands.

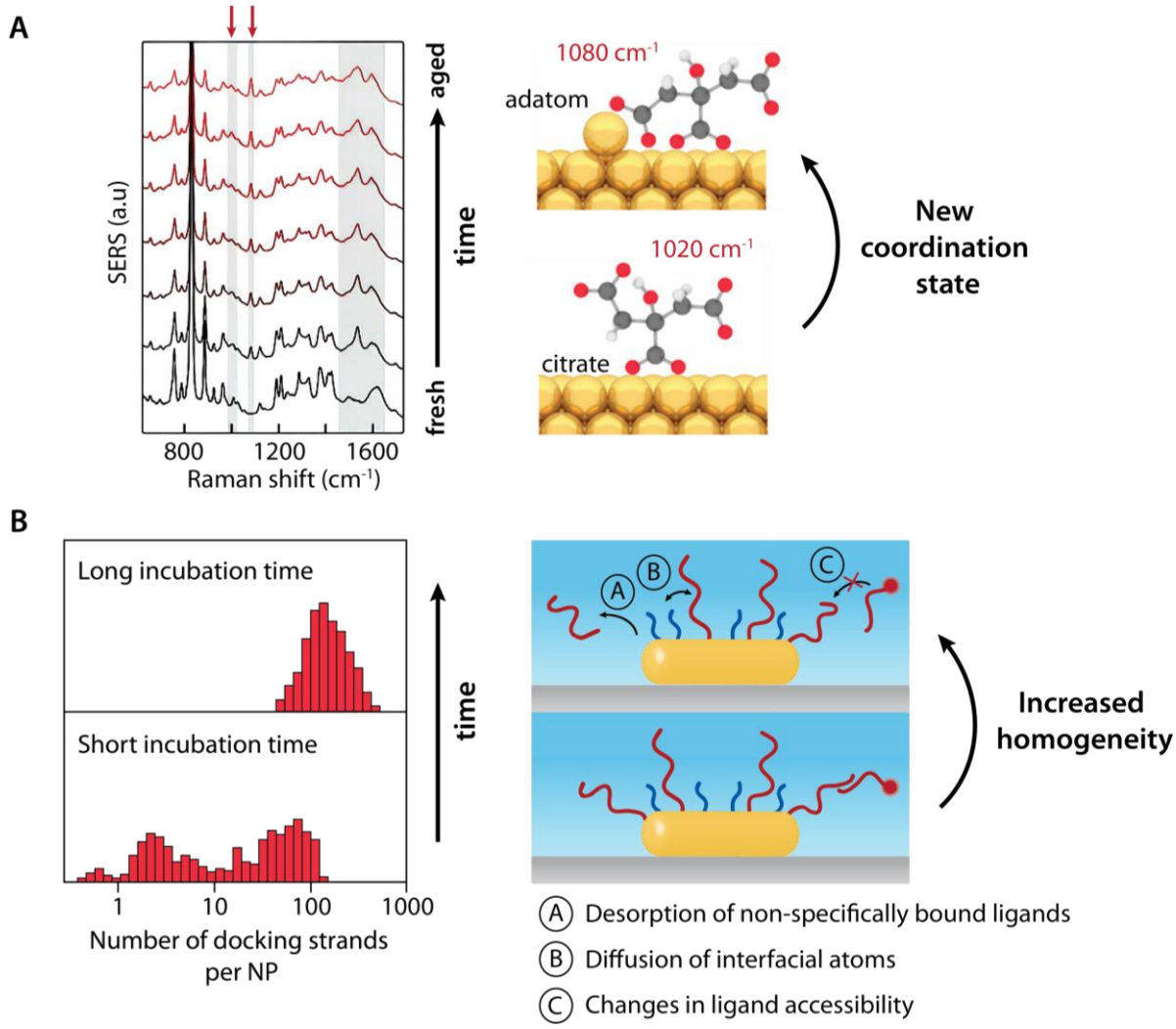

Figure 2. Spontaneous ligand reorganization and desorption. (A) Evolution of Au-citrate coordination over time, switching from single bidentate binding (1020 cm^{-1} SERS signal) to

double one (1080 cm^{-1}). The phenomenon involves the displacement of gold adatoms atop the NP surface. Adapted under terms of the CC-BY license from [59] 2020, American Chemical Society; (B) Evolution of ligand density over time. The number of DNA docking strands per NP becomes more homogeneous thanks to ligand reorganization. Adapted from [60].

3.2. Chemical degradation

In biomedical applications, NPs are frequently exposed to environments prone to trigger chemical reactions such as hydrolysis or oxidation. Apart from the inevitable exposure to water and air, some specific regions in the body can display more extreme conditions. Tumors, for instance, are considered more acidic than healthy tissues, lysosomes are characterized by very low pH, and intracellular environments contain high concentrations of redox-active molecules.[64,65]

Hydrolysis is a common chemical process taking place in biological environments. Numerous studies have taken advantage of this process to design biodegradable materials or particles. For instance, Kumari *et al.* reviewed biodegradable polymers used to synthesize polymeric NPs used for drug delivery purposes.[66] Several of them have also been used as ligands for inorganic NPs. For instance, natural polymers such as chitosan and dextran are frequently used to coat both IONPs and AuNPs, as they display high hydrophilicity and biocompatibility.[67–69] These polysaccharides can undergo acid hydrolysis through the cleavage of their glycosidic bonds.[70,71] This hydrolysis process has been hypothesized as the cause for the size reduction of dextran-coated IONPs observed after several months of storage.[72]

Hydrolysis can also affect synthetic polymer ligands, as demonstrated by Carregal-Romero *et al*.[56] The authors compared the biodistribution in mice of IONPs at two aging stages (3 weeks vs 9 months) and observed strong differences, despite similar results in routine characterization of the particles (size, shape, and zeta potential). Nuclear magnetic resonance spectroscopy (NMR) evidenced time-dependent hydrolysis of the ester groups present in the polymer coating of the NPs (originating from a pyridine-acrylate bond linking a PEG chain to the poly(4-vinyl-pyridine) coating). The authors hypothesized that this degradation was responsible for the altered *in vivo* behavior of the NPs. Interestingly, in the case of methacrylates and methacrylamides, polymers displayed stronger resistance to ester hydrolysis than the corresponding monomers.[73,74]

Some studies used hydrolytic degradations to design pH-responsive nanomaterials, as reviewed by Kanamala *et al.*[75] A variety of labile bonds can indeed undergo cleavage under acidic conditions. For instance, acetal- and ketal-containing crosslinkers were used to trigger the disassembly of polymers in acidic pH.[11,56][76,77] Acetal-derivatized dextran was also shown to undergo a hydrophobic-to-hydrophilic transition upon acetal cleavage.[78] The same polymer was later used to coat ultrasmall AuNPs encapsulated in polymeric micelles.[79] In such a pH-responsive system, cleavage of acetal bonds changed the polymer coating of AuNPs from hydrophobic to water-soluble, leading to destabilization of the micelle and release of AuNPs.

Oxidation is another commonly reported chemical process affecting ligand stability. In the case of gold, oxidation of thiolated self-assembled monolayers (SAMs) has been widely reported on planar surfaces, both in air and in solutions.[80,81] The degradation mechanism involves the conversion of thiolates into weakly bound sulfonates, which subsequently triggers ligand desorption. Photooxidation by UV has been suggested in many instances (possibly due to ozone produced by photolysis of O_2),[82] even though evidence has also been provided for oxidation in dark conditions.[83] The length of the SAM chains has been shown to impact the oxidation process, as slower degradation was observed for longer chains, probably due to the need for oxidative species to penetrate the monolayer.[84] For more details about the stability of SAMs on flat gold surfaces, we refer the reader to the review published by Srisombat *et al.* on the subject.[85]

Oxidation of thiolated SAMs in air has also been observed for AuNPs deposited on substrates, either under light exposure or in dark conditions.[81,86] The absence of light only appeared to slow down the kinetics of the phenomenon.[86] As for particle suspensions, the stability against oxidation of gold nanoclusters coated with SAMs was studied in solution through NMR spectroscopy and X-ray photoelectron spectroscopy (XPS).[87,88] A two-step oxidation process was evidenced, involving the conversion of thiol groups to disulfides and then to sulfonate groups (**Figure 3A**).[87] Rather than light, the presence of halide ions was found to be critical for this process to occur. Interestingly, lower oxidation rates were obtained for large sizes of particles. The same group later evidenced a weaker resistance to oxidation for dithiolate-protected nanoclusters compared to their monothiolated analogs.[88]

Even though most studies have been performed with alkanethiols, Bhatt *et al.* focused on the stability of AuNPs coated with thiol-modified DNAs.[89] The authors reported evidence of some

DNA degradation over time, but the primary mechanism of ligand loss was rather DNA desorption through Au-thiol cleavage, which was observed in all aqueous conditions tested. Even though no experimental proof was provided, it seems plausible to assume that oxidation of the gold-sulfur bond was the main mechanism of ligand desorption.

Ligand photooxidation has also been observed for metals other than gold and anchoring groups other than thiols. Amine-terminated SAMs have been shown to undergo photooxidation on gold planar substrates, where amino groups were turned into nitroso groups.[90] Aldana *et al.* have also demonstrated that the photochemical instability of CdSe nanocrystals coated by thiols was due to an oxidation process of the ligands catalyzed by the metallic core, where thiols were converted into disulfides.[91] Interestingly, the authors compared dithiols to monothiols ligands and observed a decreased stability for dithiols, as reported for AuNPs.[88] Two reasons were hypothesized: dithiols cannot pack as densely as monothiols on the surface of NPs, hence an easier diffusion of O_2 through the ligand shell, and dithiols are more likely to form an intramolecular disulfide bond.

Highly oxidative microenvironments are also found in living organisms, via the presence of reactive oxygen species (ROS) and reactive nitrogen species (RNS) such as hydrogen peroxide (H_2O_2), superoxide ion ($O_2^{\bullet-}$), hydroxyl radical ($^{\bullet}OH$), hypochlorite ion (OCl^-), nitric oxide (NO), and peroxynitrite ($ONOO^-$).[92] These ROS and RNS play a major role in cell signaling pathways. They are usually quickly scavenged and quenched by natural antioxidants, but high concentrations can still be found at inflammation sites or in the case of specific diseases, including some types of cancers. As a result, oxidation-sensitive chemical groups such as thioethers or aryl boronic esters have been used to develop responsive polymeric materials and NPs.[92,93] Some of these reactive species have also been proven to oxidize and degrade thiolated SAMs on gold surfaces[16][94,95] as well as to depolymerize polysaccharides in biologically relevant conditions.[96]

Reductive environments can also be encountered by NPs *in vivo*. Levels of the reductive tripeptide glutathione (GSH) are approximately 2-20 µM in the extracellular space and 2-10 mM in the cytosol and nucleus.[97] Accordingly, intracellular environments are prone to cleave reduction-sensitive bonds such as disulfides, diselenides, and succinimide thioethers.[98] Conditions of reductive stress can also be found in tumors, due to high concentrations of GSH in their microenvironment.[99,100] Yet, the lower pH found in tumors might inhibit the reduction

reaction as it favors the protonated thiol form over the reactive thiolate one.[101] These characteristics have been used to design redox-responsive nanoparticulate systems to deliver drugs in tumor tissues or inside cells.[97,98] Nevertheless, cleavage of disulfide bonds may happen in other biological compartments such as the bloodstream, even though the lower redox potential of the species found in the blood implies slower reactions compared to tumor tissues and intracellular environment.[101] As disulfides play an important role in the folding and stability of proteins, their cleavage may affect the targeting properties of peptides or antibodies attached to NPs.

As revealed by all these studies, various chemical processes such as hydrolysis and redox reactions can affect the integrity and linkage of ligands at the surface of NPs. Oxidation seems to frequently impact the anchor groups, therefore triggering desorption, while hydrolysis and reduction mostly affect the structure of ligands, especially in the case of biopolymers and biomacromolecules.

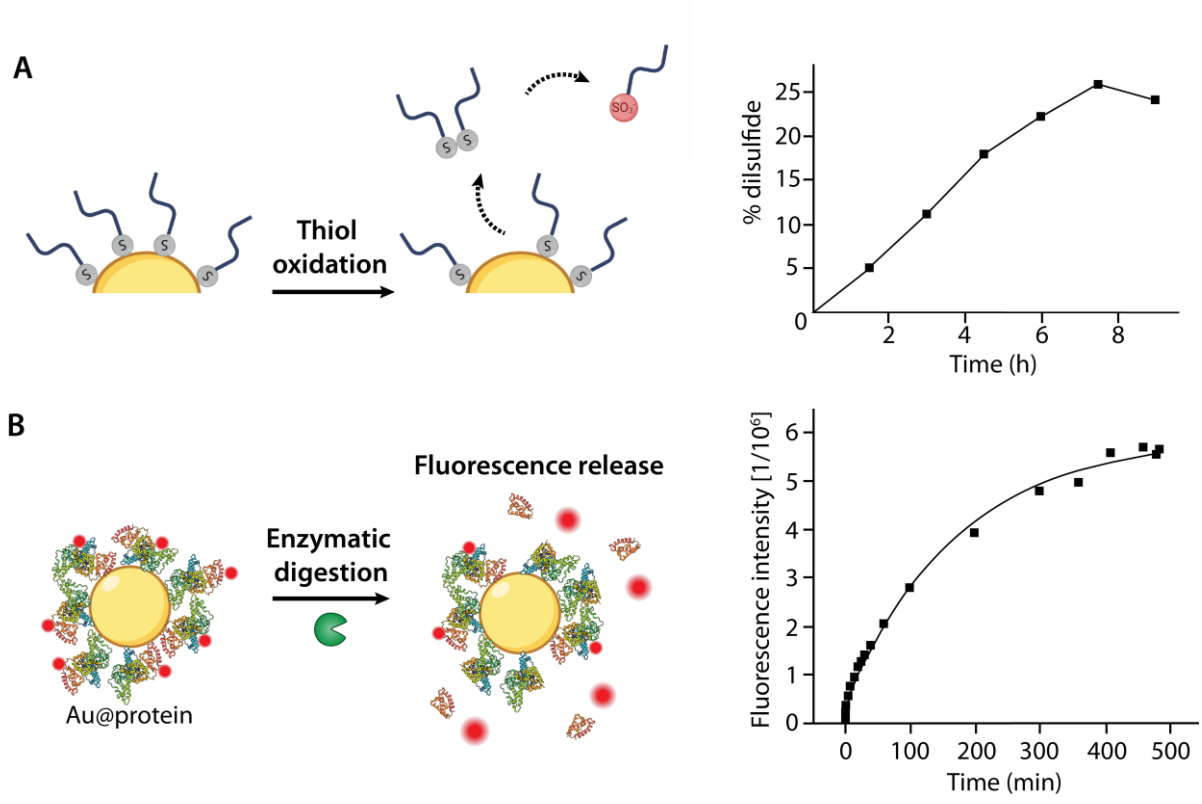

Figure 3. Examples of chemical and enzymatic ligand degradation. (A) Thiol oxidation is observed at the surface of AuNPs. Thiol groups get transformed into disulfides, which turn into sulfonates; (B) Proteins at the surface of NPs get digested by enzymes, as demonstrated by the

release of initially quenched fluorophores. Adapted with permission from (A) [87] 2007, American Chemical Society; (B) [102] 2013, Wiley Online Library. Figure created with the help of Biorender.com.

3.3. Enzymatic degradation

Hydrolytic and redox reactions can also be catalyzed *in vivo* by numerous enzymes, respectively known as hydrolases (including esterases, proteases, glycosidases, and phosphatases, among others) and oxidases or oxygenases.[103] For instance, the protein disulfide isomerase (PDI) and the thioredoxin display redox properties and catalyze the formation and breakage of disulfide bonds in proteins,[101] while lysozyme-mediated hydrolysis is considered the main degradation mechanism of chitosan.[71,104] High concentrations of such enzymes can be found in all body compartments, therefore exposing NPs to degradation.

A variety of polymers has been shown to undergo enzymatic degradation. Polysaccharides such as chitosan and dextran can be quickly hydrolyzed by multiple enzymes,[104–106] but synthetic polymers are also prone to such degradation. For instance, polyester NPs are degraded by lipases;[107] some polymethacrylates are susceptible to esterase hydrolysis;[108] while a range of enzymes is able to degrade poly (glutamic acid) (PGA) as well as to cleave amide bonds between PGA and hydrophobic side chains.[109]

Evidence of enzymatic degradation of polymer ligands on inorganic particles is scarce. Bhattacharya *et al.* demonstrated that covalently attached PEG coatings were stripped from carbon nanotubes in the presence of neutrophil proteases.[110] In another study by Zhu *et al.*, IONPs covered with a poly-(isobutylene-alt-maleic anhydride)-graft-dodecyl (PMA) shell decorated with a fluorescent dye via different chemistry bonds were exposed to multiple enzymes including trypsin, cathepsin G, lactate dehydrogenase, aminotransferase, acetylcholinesterase, proteinase K, or fetal bovine serum (FBS).[111] Potential enzymatic cleavage from the NP surface was investigated by measuring the fluorescence signal of released dyes and polymer fragments after separation from the particles. As all dye linkers contained amide bonds, the enzymes able to cleave such bonds, such as trypsin or enzymes present in FBS, were logically found to trigger the release of the dye. However, it was found that certain enzymes were able to release the dye only when specific conjugation chemistries were used. A previous study with the same polymer grafted on AuNPs had also confirmed enzymatic degradation by a range of enzymes.[45]

Most biological molecules can also undergo enzymatic degradation, even when used as NPs ligands. Digestion of albumin coating on poly(lactic acid) NPs was demonstrated in simulated gastric and intestinal fluids;[112] insulin and ovalbumin coatings on AuNPs were shown to undergo enzymatic digestion by pronase, whether or not the NPs were agglomerated (**Figure 3B**);[102] and cleavage of peptides on AuNPs was evidenced in the presence of thrombin.[113] Böttger *et al.* also showed the differential stability of free peptides in serum, plasma, and fresh blood due to proteolytic degradation.[114] These studies point out an under-estimated issue, *i.e.*, the limited chemical stability of peptides and proteins in biological fluids, which limits their use as targeting ligands. Yet, Seferos *et al.* evidenced an interesting protective effect of AuNPs towards the enzymatic cleavage of grafted DNA strands compared to free DNA.[115] Their results indicated that AuNPs did not prevent enzyme binding to DNA but rather slowed down the hydrolytic degradation, thanks to high local concentrations of salts inhibiting the DNase.

As observed for chemical degradation, the action of enzymes has been used to design responsive drug delivery systems. The different strategies were summarized in various reviews.[116,117]

These studies show that the presence of multiple enzymes in biological environments may further limit the stability of ligands, as these enzymes can catalyze different types of reactions. Specific attention should be given to the case of biomacromolecules, which are widely used to add functionalities to NPs but whose stability might be challenged *in vivo*.

3.4. Ligand exchange

3.4.1. Surface fine-tuning vs unsolicited modification

Nanoparticles intended for medical applications must be stable in biological media and biocompatible. To tune these properties, it is often necessary to modify their surface chemistry post-synthesis. For this purpose, one popular strategy is ligand exchange, *i.e.*, the replacement of a pre-existing ligand used specifically during the synthesis step by a new ligand aimed to provide biocompatibility to the NP. This process also enables coating the NP surface with drugs, dyes, or targeting moieties.[118,119] The first ligand exchange reaction on NPs was reported by Murray *et al.* in 1996, where the authors performed an exchange reaction of thiolated ligands on monolayer-protected gold clusters.[120] This strategy has since been widely used to modify the AuNP surface.[121] Indeed, one of the most common syntheses of AuNPs is the Turkevich

method,[122] which generates citrate-coated AuNPs that are often considered unstable in biological media and more toxic than AuNPs with other surface coatings. An alternative method is the Brust method, which allows synthesizing AuNPs directly in the presence of thiolated ligands,[123] but which only results in small (diameter < 10 nm) and rather polydisperse AuNPs. Surface modification of NPs is also required for AuNRs, as their synthesis involves CTAB, a molecule known to be highly toxic.[124] Thus, to use AuNRs in the medical field, it is essential to proceed to complete ligand exchange to replace CTAB. This kind of process is also used for NPs other than AuNPs. For instance, IONPs require ligand exchange since most syntheses produce hydrophobic particles.[125–127] Furthermore, the surface coating can reduce IONP toxicity by decreasing the number of oxidative sites liable to generate cellular oxidative stress.[128] Synthesis of QDs and upconverting NPs requires the use of hydrophobic ligands as well. Post-synthesis replacement is therefore necessary for their use in biological media.[49,129,130]

Ligand exchange with biomolecules can also occur when NPs are introduced into a biological environment. Biogenic thiols and disulfides such as GSH, dihydrolipoic acid, cysteine, and cystine can be responsible for the displacement of ligands at the NP surface. Multiple studies showed that these biogenic thiols can displace various thiol ligands from the surface of AuNPs.[131–135] *N*-heterocyclic carbene ligands, which are considered alternatives to thiols, did not display better stability against GSH exchange.[136] Conversely, polymer ligands grafted on QD surface through multiple imidazole anchoring groups were shown to resist exchange with GSH.[137] Exchange can also happen with free proteins, as in the case of carbon nanotubes, where proteins displaced adsorbed DNA strands.[138] On the contrary, antibodies with a strong affinity for AuNP surface could not be displaced by plasma proteins.[139] Exchange may also occur with thiols from immobilized proteins, for instance proteins constituting the extracellular matrix or proteins expressed on the surface of cells (such as the protein disulfide isomerase found on endothelial cells[101]). Finally, ligand exchange was also shown to take place with lipids during interaction with the cell membrane, as demonstrated by Wang *et al.*[140] Interestingly, simulations evidenced that the presence of defects in the SAM structure of metal NPs provides sites for phospholipid extraction.[141] This type of exchange is expected to have an impact on the NP endocytic pathways and uptake efficiency, as well as on the integrity of the cell membrane.

3.4.2. Mechanisms of ligand exchange

Two main exchange pathways have been reported in the literature (**Figure 4A**). The first is the associative mechanism, where the incoming ligand co-adsorbs on the NP surface with the initial ligand before triggering its release (equivalent to a type 2 nucleophile substitution, S_N2, reaction mechanism in organic chemistry). This process implies a first-order dependence on the concentration of both the incoming and initial ligand. It has been demonstrated to be the predominant pathway in the case of thiol/thiol exchange.[48,142–144] The second mechanism is the dissociative pathway, which first involves spontaneous desorption of the initial ligand, followed by the adsorption of the incoming ligand (equivalent to an S_N1 mechanism). This process is therefore independent of the concentration of incoming ligand. Ligand exchange of thiol-protected AuNPs *vs* disulfides was shown to undergo such a mechanism, where the S-S bond is cleaved during adsorption.[145,146] Ionita *et al.* observed the non-adjacent adsorption of the two branches of the disulfide on the NP surface[145] and later suggested that only one branch gets adsorbed, while the other one associates with the exiting ligand to form a mixed disulfide.[146] The same group also demonstrated a dissociative mechanism in the case of ligand exchange between AuNPs.[147] Coexistence of the two pathways can take place, as shown by Song *et al.* for thiol exchange under oxidizing conditions.[148] More complex mechanisms have also been hypothesized.[149]

Several studies have reported the coexistence of two rate constants in the ligand exchange process, corresponding to fast and slow exchange.[142,143,150,151] This observation is consistent with binding sites exhibiting different reactivity. Fast exchange was hypothesized to occur on low coordinated sites, such as vertexes, edges, and defects, whereas high coordination sites such as terraces are considered less reactive, undergoing slower exchange, as schematized in **Figure 4B**.[142,146,151] The fact that incomplete exchange is frequently observed[48,142,149,152–155] has also been suggested to be caused by this difference of reactivity, where only the low coordinated sites are exchanged.

Regarding the morphology of the ligand shell during ligand exchange, Luo *et al.* observed at the surface of spherical AuNPs an initial random distribution which later evolves into a patchy morphology.[156] Interestingly, the authors showed that the ligand shell morphology kept evolving even after the ligand composition had reached a plateau. The same group later performed a similar analysis on silver nanocubes which exhibited two different behaviors,

depending on the chemical nature of the incoming ligand.[157] Random distribution was observed when a hydrophilic ligand was used, while ligand exchange proceeded via the formation of island nanodomains for the more hydrophobic ligand.

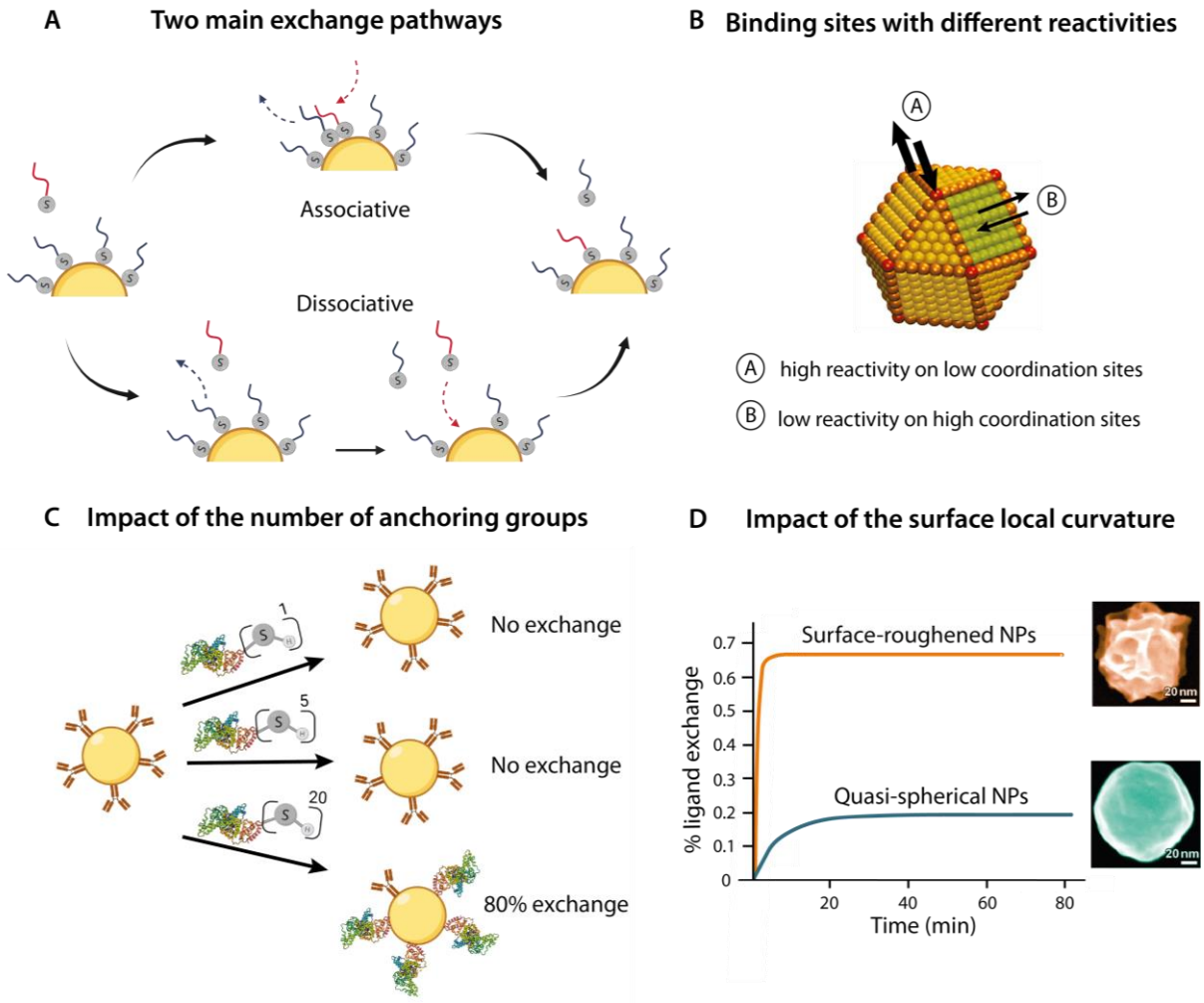

Figure 4. Mechanisms of ligand exchange and examples of key properties affecting the process. (A) Two main exchange pathways have been reported for ligand exchange, the associative pathway and the dissociative pathway; (B) Binding sites at the NP surface display different reactivities: low coordination sites (*i.e.*, vertexes, edges, and defects, represented in red) are more reactive than high coordination sites (terraces, represented in blue); (C) The number of anchoring groups on the incoming protein has a great impact on the extent of ligand exchange with the antibody initially on the NP surface (presence of 1, 5, or 20 free thiols); (D) The NP local surface curvature influences the kinetics and extent of the ligand exchange process. Comparison of surface-roughened and spherical nanoparticles shows higher and quicker ligand exchange for the surface-roughened ones. Adapted with permission from (C) [158] 2020,

American Chemical Society; (D) [149] 2017, American Chemical Society. Figure created with the help of Biorender.com.

3.4.3. Parameters affecting ligand exchange

Two classes of parameters can impact the efficacy of ligand exchange: the intrinsic parameters, *i.e.*, ligand and NP properties (charge, size, chemical nature, grafting density), and the extrinsic parameters (solvent, pH, temperature, concentration). NP aging was also proven to be influencing ligand exchange, as previously mentioned.[58,159] It is noteworthy that most studies about the parameters affecting ligand exchange reported on AuNPs. Very few studies have addressed this phenomenon on other inorganic NPs.

Ligand properties

The properties of both the initial and incoming ligands have been shown to play a key role in the ligand exchange process. For instance, the impact of ligand length has been studied in multiple conditions. One of the earliest studies about place-exchange reactions on gold nanoclusters, published by Hostetler *et al.* in 1999, showed a lower reaction rate and extent for increased chain length and/or steric bulk of the initial alkanethiol ligands.[48] The authors explained this result by the presence of chain-chain interactions stabilizing the monolayer. The recent thermodynamic study by Calvin *et al.* on ligand exchange at the surface of QDs confirmed the positive contribution of alkyl chains interactions on monolayer stability.[160] Wang *et al.* obtained similar results for ligand exchange experiments involving lipid bilayers and AuNPs coated with physisorbed DNA strands of various lengths.[140] Molecular dynamics simulations demonstrated higher layer thickness and binding energy with increasing strand length, two features that hinder ligand exchange according to the authors. The opposite trend was observed by Smith *et al.* who compared the ligand exchange efficiency for AuNPs functionalized with either macromolecules or small molecules of different chemical structures.[161] For both 13nm and 30nm AuNPs, 70 to 95% of initial PEG-SH ligands were displaced by small thiolated molecules. Meanwhile, PEG-SH was found unable to displace the initial 3-mercaptopropionic acid and 11-mercaptoundecanoic acid. The authors partly explained this size effect by the difference in grafting density, with the PEG layer being less densely packed and therefore more subject to displacement. Favorable intermolecular interactions between carbon chains were also hypothesized to be an important parameter. Regarding the size

of the incoming ligand, simulations showed that low molecular weight PEG was better at displacing CTAB from AuNP surface compared to PEG with higher molecular weight, thanks to better diffusivity.[162] This effect of diffusion was also reported at the surface of QDs while exchanging oleic acid with alkylamines of varying lengths.[163] The thermodynamic study of Liu *et al.* revealed that three phenomena were at play: Van der Waals interchain interactions, steric barrier, and diffusion rate. Short-chained incoming ligands reach more easily the NP surface thanks to a higher diffusion coefficient and reduced steric barrier, while long-chained ligands provide greater stability to the resulting coating thanks to stabilizing interactions among alkyl chains. The authors tested three chain lengths and obtained higher ligand exchange for the intermediate length, highlighting the balance between these phenomena.

The nature of the anchoring group, and thus the ligand/NP binding energy, are also greatly influencing ligand exchange. Ionita *et al.* demonstrated that phosphine-protected AuNPs underwent ligand exchange to a much greater extent than thiol-coated AuNPs, presumably due to weaker interaction with gold.[146] The functional group chemistry of the incoming ligand was also shown to determine the kinetics and efficiency of exchange, with thiolated molecules demonstrating a higher ability to displace citrate on the surface of AuNPs, compared to amine- or carboxylate-containing molecules.[164] Thiolated DNA strands were also much more resistant to exchange on AuNPs than their physisorbed counterparts, thanks to their higher grafting density and binding energy.[140] The anchoring group was also shown to impact the extent of ligand exchange at the surface of IONPs.[127] A molecule can also present different binding energies depending on its binding mode (and therefore grafting density), as shown for citrate, which may change from easily displaced monocarboxylate monodentate linkage at high coverage to a more stable dicarboxylate anchoring at low coverage.[164] As a result, an unexpected increasing resistance to displacement was observed for citrate at low coverage. The effect of the coordination number was also studied for other types of ligands. Three studies compared the stability of monothiol- *vs* dithiolane-functionalized PEG ligands on AuNPs and showed a better resistance to displacement by dithiothreitol for the bidentate ligand.[13,165,166] Similar results were obtained for IONPs, with bifunctional sulfonate and phosphonate moieties providing better stability than their monodentate counterparts.[127] Oh *et al.* furthered the analysis by comparing flexible dithiol, constrained dithiol, and disulfide anchoring groups on AuNPs.[13] Their results showed that ligand stability can be enhanced using anchoring groups with constrained and compact structures, which favor dense packing on the NP surface. Similar

results were obtained with thiol- and disulfide-ended DNA strands.[167] Awotunde *et al.* also studied the effect of multidentate binding by comparing human serum albumin (HSA) molecules modified to present 1, 5, or 20 free thiols.[158] The authors pre-adsorbed on AuNPs an antibody exhibiting 10 free thiols. No exchange was detected with the HSA presenting 1 or 5 free thiols, whereas the one with 20 free thiols was shown to displace 85% of the antibody (**Figure 4C**). Likewise, when HSA was pre-adsorbed on AuNPs, only the one with 20 thiols resisted the exchange with the antibody. The authors concluded that the interaction between AuNPs and their biomolecule ligands was governed by the number of Au-S bonds.

The whole chemical structure of the ligands may also impact ligand exchange, through steric hindrance and interchain interactions, for instance. Hong *et al.* observed the displacement of thiol ligands by primary, secondary, and tertiary thiols and showed that primary thiols were the most efficient.[168] However, if a bulky group is placed 1 or 2 carbons further from the thiol, branched thiols exhibited higher displacement efficiency. The authors explained this phenomenon by the fact that place exchange mainly occurred at vertices and edges of the particle, where the monolayer is less densely packed. They also suggested that branched thiols could pack better than linear ones and that their bulkiness was further destabilizing the initial thiols around. Interestingly, the same authors showed that a racemic thiol mixture was more efficient at triggering ligand exchange than the analogous homochiral thiol, thanks to better packing.[168] The spacer structure was further studied by Schulz *et al.*, comparing PEG ligands with different segments connecting them to a thiol anchor.[166] A long alkyl spacer was shown to provide better resistance to DTT-induced displacement compared to a short one, and both alkyl spacers yielded greater stability than the phenyl one. The long alkyl spacer was thought to prevent ligand exchange by creating a thicker inner hydrophobic layer and by improving the PEG grafting density thanks to better packing. Goldmann *et al.* later demonstrated the importance of intermolecular chain interactions in the ligand exchange process.[169] Through experiments and density functional theory (DFT) calculations, the authors investigated a series of ligands with different chain structures: one alkanethiol (dodecanethiol (DDT)) and 3 arylthiols (containing 1, 2, or 3 aromatic phenyl groups). For the latter, ligand affinity for the surface was found to increase with the number of aromatic groups. This stabilization of the monolayer for longer aryl chains was demonstrated to originate from increased attractive interchain interactions (including π stacking). This study also showed the role of the chain structure, with DDT being resistant to displacement by arylthiols despite lower entropy. Again,

the predominant role of intermolecular interactions (dispersion type in the case of DDT) was evidenced. The impact of the ligand bulkiness was also studied by Gao *et al.*, where simulations showed that polystyrene was less efficient at displacing CTAB compared to PEG chains of similar length, as its larger size and higher rigidity limit its penetration into the CTAB layer.[162]

The terminal group of the ligands can also play a major role in ligand exchange. Chompoosor *et al.* investigated the impact of particle surface charge on the stability of AuNP ligands upon exposure to biogenic thiols.[132] The authors synthesized a series of AuNPs with different surface charges (from +30 mV to -36 mV), using mixtures of ligands with positively charged, negatively charged, or neutral terminal groups. All NPs were labeled with fluorophores initially quenched by the NP. Upon treatment with a GSH solution, ligand displacement was quantified through fluorescence recovery. Fluorophore release was shown to increase when the NP surface charge was positive whereas no release was observed for negatively charged AuNPs. The hypothesis put forward was the electrostatic repulsion between the NP surface and the anionic GSH molecules. Smith *et al.* also demonstrated a stronger capacity of carboxylic acid-terminated alkyl ligands to displace PEG-SH ligands compared to their amine-terminated equivalent.[161]

NP properties

The effect of core size (and therefore surface curvature) on ligand exchange has been investigated in various studies. Guo *et al.* showed a higher thiol exchange on Au_{38} clusters compared to Au_{140} clusters,[170] and Kluenker *et al.* obtained similar results exchanging oleylamine by one alkanethiol on AuNPs.[153] Nevertheless, Goldmann *et al.* reported an increased exchange efficiency on larger NPs in the case of DDT displacement by an aryl thiol.[169] The latter result was explained by a lower entropy of the initial layer (better packing of DDT on large NPs) and by increased favorable interchain interactions in the resulting layer (rigidity of the aryl ligand preventing these interactions on smaller NPs). Villarreal *et al.* used nanotextured AuNPs to study the impact of local surface curvature independently of the core size.[149] They compared the ligand exchange of thiolated aromatic ligands on surface-roughened NPs (SRNPs) *vs* quasi-spherical NPs (QSNPs) of similar size. Exchanged amounts were found to be higher on the SRNPs (72% *vs* 20%) (**Figure 4D**). The authors hypothesized that only the ligands located on highly curved regions were exchanged, highlighting the key role of local surface curvature on ligand exchange. Interestingly, this result is consistent with

the hypothesis of a higher reactivity for low coordinated sites, as already mentioned in the section dedicated to mechanisms.

The charge of the core can also impact ligand exchange, as demonstrated by Song and Murray.[142] Both the rate and extent of ligand exchange between two thiols on gold nanoclusters were shown to increase when the core was positively charged.

Recently, the effect of the core shape on ligand exchange has been investigated with DFT calculations by Chan *et al.*, comparing gold nanoclusters with a sphere, rod, or star shape.[171] The authors observed that the presence of PEG ligands significantly improved the stability of the stellated nanocluster, even inducing some further stellation. This higher stability implies a larger energy cost to desorb the ligands, compared to more spherical cores, which provides better resistance to ligand exchange. The intrinsic stability of the object was also demonstrated to be driving the direction of ligand exchange, either through simple ligand exchange or through other structural transformations (such as aggregation).[172]

Lastly, the chemical nature of the inorganic core is a parameter that impacts ligand exchange by changing the affinity of the ligands for the surface. Qing *et al.* reported that the Pt-S bond is much more stable than the Au-S bond.[173] They demonstrated that Au@Pt NPs (*i.e.*, AuNPs covered with a thin layer of platinum) do not undergo exchange with GSH, contrary to AuNPs.

Environmental conditions

Early demonstration of the impact of the environmental conditions on ligand exchange was provided by Song and Murray.[142] They showed that acid-base conditions, O_2 presence in the atmosphere, and solvent polarity could affect the dynamics and extent of the place exchange reaction of thiolated ligands at the surface of gold nanoclusters. The decrease in reactivity observed in acidic conditions suggested that thiolates are more reactive than the corresponding thiols. The pH was also found to play a critical role in the displacement of citrate by various pesticides on AuNP surface.[174] Overall, this impact depends on the pKa of the exchanged species, and therefore on the protonation and deprotonation of functional groups. This was studied in detail on cadmium-containing quantum dots by Lesiak *et al.*, using an incoming ligand that contained carboxyl, amine, and thiol functional groups, and testing four pH to probe its different protonation states.[175] Simulations performed by Gao *et al.* also confirmed that the solvent could affect both the surface packing of the initial ligand and the diffusivity of the incoming one, hence a strong impact on the ligand exchange process.[162]

As expected with the associative mechanism, the concentration of the incoming ligand was also shown to influence ligand exchange. Goldmann *et al.* observed a greater ability of arylthiol to displace DDT from AuNP surface at high concentration and hypothesized the phenomenon was due to an equilibrium displacement related to the maximum solubility of the ligand.[169] The same trend was obtained with simulations of CTAB displacement by PEG-SH.[162] This result also seems in line with the greater displacement observed for repeated reactions performed with a large excess of incoming ligand.[153]

The phenomenon of ligand exchange has been one of the most studied in the field of ligand stability. Initially used for functionalization purposes, this process was shown to occur *in vivo* as well, where the great diversity of biological molecules increases the probability to find one with a high affinity for the NP. Studies on the subject have helped identify the underlying mechanisms and key parameters in controlled environments, but more studies are needed to understand the phenomenon *in vivo*.

3.5. Degradation or desorption under external stimuli

When exposed to an external stimulus, inorganic NPs can display various intrinsic properties that can be used for therapeutic purposes. For instance, NPs may generate hyperthermia upon exposure to a magnetic field or electromagnetic radiation, or they can enhance the toxic effects of ionizing radiations, a property used in radiosensitization. Organic ligands located at the surface of the core of the NPs can thus be impacted by these effects, especially since most of them imply surface phenomena. However, very few studies have tackled the subject, and the issue is rarely mentioned in the nanomedicine literature. In this section, we describe how the different external stimuli used to trigger NP therapeutic effects may cause degradation or desorption of the ligands.

3.5.1. Plasmon-driven effects

Thanks to the phenomenon of localized surface plasmon resonance (LSPR), metallic nanostructures can display unique optoelectrical properties leading to fast heating under excitation at a specific wavelength. This photothermal effect has been investigated for medical applications, to treat tumors through locally elevated temperatures. Various types of NPs have demonstrated such properties, among which are gold nanoshells and nanorods.[176] Yet, the fate of ligands during photothermal treatment has not been considered, even though the physical

phenomena involved in LSPR may affect them, as we will show in this section. It should be noted that the impact of the plasmon-generated heat will be treated in a second section dedicated to the effects of hyperthermia.

Over the last decades, plasmons have been shown to induce various chemical reactions at the surface of NPs, from polymerization to photochemical or photocatalytic reactions, opening a new research field about plasmon-mediated chemical reactions. The first report of such a reaction was published in 1983.[177] Multiple reviews have since described the advances of this still-expanding field.[178–182] Interestingly, plasmon-driven reactions have also been shown to offer a strategy to trigger site-selective surface functionalization to place molecules into specific reactive spots, as recently reviewed by Kherbouche *et al.*[183] Therefore, the possibility to induce chemical reactions with surface plasmons (SPs) highlights how the exposure of surface ligands to this phenomenon may affect them and generate instability.

Upon excitation and relaxation of SPs in plasmonic NPs, three main successive processes can take place: local electromagnetic field enhancement, emission of both photons (radiative decay) and hot carriers (non-radiative decay), and heat dissipation.[180] All these processes can participate in plasmon-driven reactions. Brooks and Frontiera studied the plasmon-driven photoreaction of 4-nitrobenzenethiol (4-NBT) to 4,4′-dimercaptoazobenzene (DMAB).[185] The authors used nanospheres deposited on a substrate and covered with a gold film to probe the rate and yield of the reaction as a function of the SERS enhancement factor. Fast formation of DMAB was observed (after 1-second irradiation), but additional pathways were also evidenced. Indeed, the loss of the 4-NBT SERS signal observed after the end of the reaction was attributed to the degradation or desorption of a portion of the 4-NBT molecules (**Figure 5A**). The same phenomenon was also observed for the produced DMAB. The photodegradation pathway was found to compete with the photochemical conversion of 4-NBT to DMAB in nearly all the regions probed, irrespectively of the SERS enhancement factor. Higher rates were measured for photoreaction compared to degradation. These results highlight the possible photodamage of ligands located at the surface of plasmonic NPs, especially in the case of extended irradiations.

Another study investigated the plasmon-driven photochemistry of 4-aminobenzenethiol (4-ABT) at the surface of plasmonic AuNRs in the presence of CTAB, citrate, or no surface ligands.[186] In the two latter situations, SERS data showed that 4-ABT was transformed into

DMAB. However, for CTAB-coated AuNRs, a new vibrational band indicated the formation of another product species, 4-NBT, through 4-ABT oxidation. Interestingly, CTAB was also found to enable the reduction of 4-NBT to 4-ABT. The authors hypothesized that the presence of CTAB increases the number of hot electrons, which induces a higher concentration of activated oxygen molecules. In another study, the presence of CTAB as a coadsorbate was shown to favor one mechanism of plasmon-driven reaction over another and, as a result, to induce product selectivity.[187] These works demonstrate once again that surface ligands not only can be impacted by plasmon-driven reactions but also that they are able to influence the reactivity of plasmonic surfaces.

Plasmon-mediated degradation of organic molecules at the surface of plasmonic NPs was further demonstrated in the context of the degradation of micropollutants in water by solar illumination.[188] Wei *et al.* first showed that citrate was degraded at the surface of AuNPs under plasmon resonance illumination, possibly via hot holes-driven oxidation. The authors also designed Janus AuNRs partially coated with silica and investigated the mechanisms underlying the degradation of organic molecules at their surface. Multiple effects were revealed: mediation of electron transfer, bulk photothermal heating, and localized effects such as higher local temperatures and hot electron generation. An earlier study by Huschka *et al.* had already identified hot electrons as responsible for dehybridization under plasmon illumination of double-stranded DNA located onto AuNP surface, in temperature conditions well below the DNA melting temperature.[189]

3.5.2. Thermal effects

Bulk thermal treatments have been shown to enable desorption of thiols[48] or dehybridization of double-stranded DNA[189] at AuNP surface. Accordingly, NP-based heating treatments are expected to produce similar results. The heating produced by the photothermal effect in metallic NPs is the result of the non-radiative decay of SPs, while magnetic materials produce heat by relaxation losses due to hysteresis when they are exposed to an alternating magnetic field.[3] In both cases, the heat is dissipated from the NP to the surrounding environment, resulting in a temperature increase. Locally, the temperatures can reach extremely high values, depending on the conditions of the stimuli. Both experiments and simulations reported surface temperatures over 100 and even 200°C in the case of plasmonic AuNPs and AuNRs under continuous and pulsed laser illumination.[190–193] Incidentally, in liquid environments, local formation of a

transient nanobubble may result from this heat generation.[190] The heat generated by the NP can therefore damage nearby molecules, such as grafted dyes or drugs, but also the surrounding biomolecules. For most proteins, denaturation indeed occurs between 45 and 65°C, and the process is found irreversible at high temperatures.[194] Nucleic acid melting temperatures may also be easily reached, as demonstrated for plasmon resonance illumination of AuNRs and nanoshells, where dehybridization of double-stranded DNA was reported.[189]

A small number of studies addressed the effect of NP-based heating on the molecules attached to the NP surface. Zeng *et al.* investigated the temperature at the surface of AuNP aggregates during photothermal effect.[195] They used photothermal heterodyne imaging to measure the absorption cross-sections of the aggregates and then calculate the local temperature rise. For single NPs of 80 nm diameter immersed in water and irradiated at 532 nm, the local temperature was predicted to reach around 60°C, while 100-250°C was estimated for aggregates of 2 to 12 NPs. The SERS signal of 4-cyanobenzenethiol ligands was also monitored under laser irradiation and was shown to be greatly reduced. According to the authors, this loss in SERS intensity may be due to molecular desorption or NP sintering.

Indeed, some chemical bonds were shown to undergo cleavage upon photothermal heating of plasmonic NPs. For instance, thermal instability of the Au-S bond was demonstrated first for bulk heating[167] and later for AuNR-generated photothermal effect.[196] Photothermal activation of the retro-Diels-Alder reaction was also used to break bonds and trigger the release of molecules from NP surfaces.[197–199] Another release strategy was used by Huang *et al.*, who embedded a model drug into polyelectrolyte multilayers wrapped around AuNRs.[200] Upon laser irradiation, photothermal heating triggered dye release thanks to decomplexation from the polymers as well as thermal expansion of the polyelectrolyte layers.

Lin *et al.* explored the possibility to trigger either desorption or adsorption of molecules upon heating, as suggested by Le Chatelier's thermodynamic principle for exothermic and endothermic reactions, respectively.[201] The authors used two different pairs of protein and polyelectrolyte-wrapped AuNRs, which display either endothermic or exothermic complexation reactions. They were able to verify experimentally the predictions obtained with Le Chatelier's principle: adsorption of bovine serum albumin (BSA) and desorption of lysozyme proteins upon photothermal heating.

These two contrasting effects might partly explain the significant variations of the protein corona (PC) composition of AuNRs observed by Mahmoudi *et al.* upon heating.[202] Yet, the authors compared conventional bulk heating to photoinduced heating and obtained distinct compositions of the PC. They hypothesized that these differences might originate from higher localized temperatures at the surface of the plasmonic AuNRs. The same group reported similar observations for the PC composition of superparamagnetic zinc ferrite spinel-graphene nanostructures and PEGylated AuNRs.[203,204] The latter system highlights that this plasmon phenomenon can reach distal regions around the NP, as PC may be affected even in the presence of a polymer shell. Conformational changes of proteins adsorbed on AuNRs induced by plasmonic heating were also evidenced.[204] Interestingly, the modified PC was found to alter the biological behavior of NPs, as cell uptake, cytotoxicity, and ROS production were different between laser-irradiated and non-irradiated PC-coated NPs.[203–205] Different observations were reported for gold nanoprisms and BSA.[206] The photothermal effect did not induce significant changes in the secondary structure of the adsorbed BSA, but Raman spectroscopy revealed a small effect on the disposition of residues close to the NP surface. The authors also reported that plasmonic heating did not supply enough energy to promote the dissociation of S-S bonds in the protein. Conformation modifications caused by plasmon heating were also observed for molecules other than proteins. Cheng *et al.* demonstrated an evolution of thiolated DNA strands on AuNR surface from a collapsed geometry to an upright and ordered one upon laser illumination.[207] The authors hypothesized that the localized heating enabled to overcome the activation barrier. Spatial heterogeneity suggested nonuniform plasmonic heating.

Several studies focused on the effects of plasmonic heating generated upon nano- to femtosecond pulsed laser illumination. Such short excitation was shown to induce a highly local and transient temperature increase.[208] Multiple studies used this effect to trigger the release of thiolated single- or double-stranded DNA from the AuNP surface.[209–212] Two mechanisms were identified, depending on the irradiation conditions: thermal DNA denaturation for low pulse energy, and cleavage of the Au-S bond for increased energy. The latter phenomenon was hypothesized to originate either from thermolysis of the bond[210] or from hot electron transfer resulting from plasmon decay[209,213]. Pulsed laser illumination was also shown to cause selective unfolding and inactivation of proteins in the vicinity of AuNPs,[191] as well as conformation transition of PEG thiols from a compact helical structure to an elongated form.[214]

The effect of magnetic hyperthermia was reported in one study, where the authors designed porous IONPs loaded with a drug and coated by a PEG protective shell for triggered delivery of chemotherapeutics.[215] Upon exposure to an alternating magnetic field, the high thermal energy generated by the superparamagnetic cores allowed to desorb the grafted polymer, triggering drug release (**Figure 5B**).

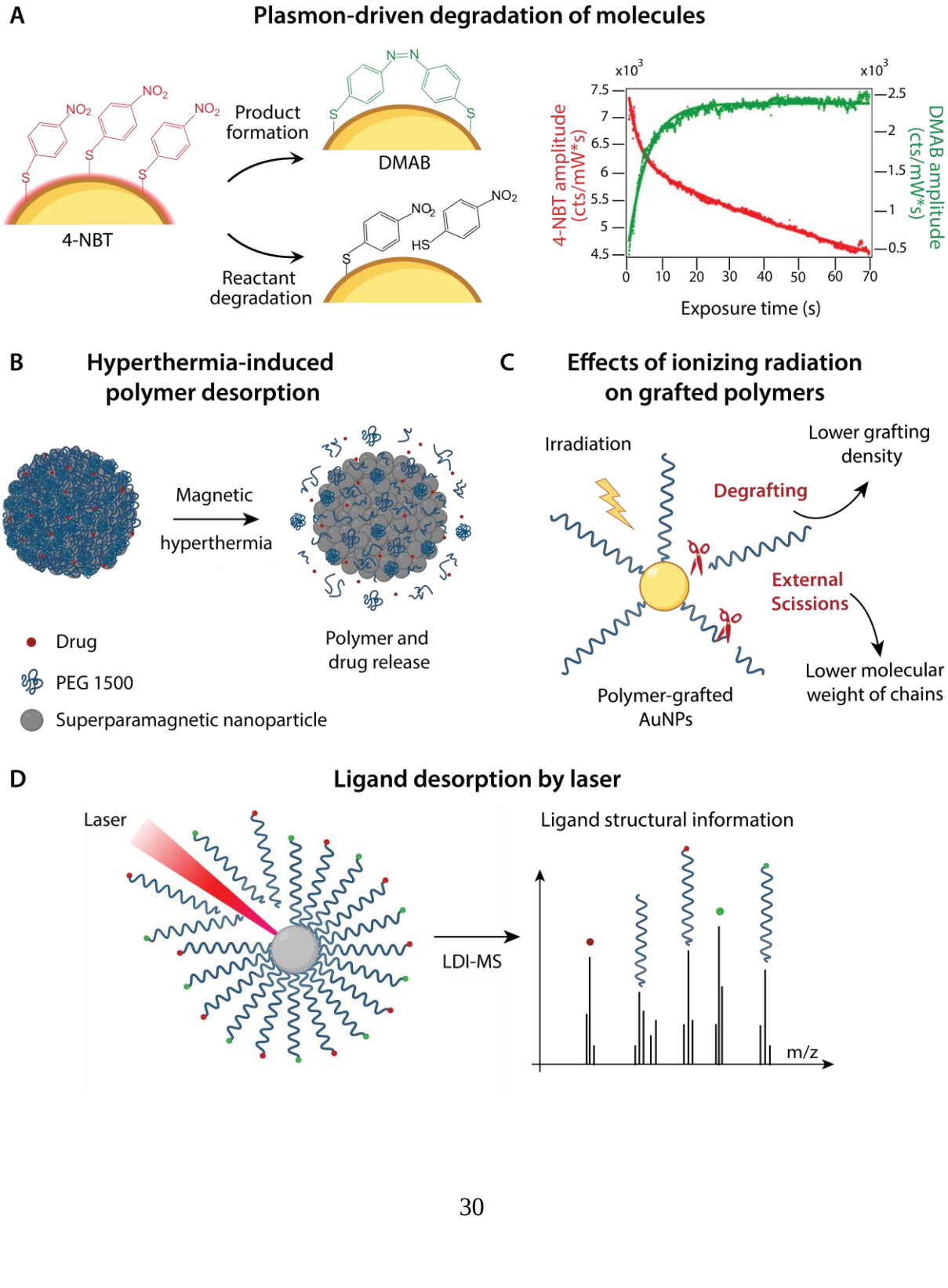

Figure 5. Ligand degradation or desorption under external stimuli. (A) Plasmon-driven conversion of 4-NBT to DMAB and degradation/desorption of 4-NBT at the NP surface. The graph shows how the 4-NBT reactant amplitude quickly decreases with concurrent growth of the product amplitude. At longer times, the reactant peak experiences a continuous decay, while the product amplitude remains constant. Adapted with permission from [185] 2016, American Chemical Society; (B) Magnetic hyperthermia is used to trigger the release of PEG ligands grafted on IONPs, and therefore of the drug encapsulated in the porous cores. Adapted from [215]; (C) Ionizing radiations can degrade polymer ligands grafted at the surface of AuNPs. Both degrafting processes and external scissions are observed. Adapted from [216]; (D) Laser-induced desorption and ionization of ligands are used in combination with mass spectrometry to enable characterization of ligand structure and composition. Adapted from [217]. Figure created with the help of Biorender.com.

3.5.3. Effects of ionizing radiations

Organic molecules and biomolecules in solution can undergo degradations upon exposure to ionizing radiations, either by direct action of radiation, interaction with the secondary electrons generated, or interaction with reactive species produced by water radiolysis. For instance, multiple behaviors were reported for polymers: scission, crosslinking, formation of small molecules, and modifications of composition and structure.[218] X-ray irradiation was shown to induce the desorption of SAMs composed of alkanethiols on a gold surface and the role of secondary electrons was evidenced.[219] Considering the common use of ionizing radiations in sterilization procedures,[220] damages induced on ligands may be highly detrimental to the properties of NPs intended for medical applications.

Additionally, metal NPs have demonstrated the ability to increase the toxic effects of the ionizing radiations used in cancer radiotherapy treatments, an effect called radiosensitization.[2,221] The underlying mechanisms are multiple and involve a combination of physical, physicochemical, chemical, and biological processes which are not yet fully understood.[222] Large amounts of secondary electrons are involved, and surface-localized processes are thought to play a major role, highlighting possible additional effects on ligands upon irradiation. For instance, plasmon excitation has been hypothesized as a possible radio-enhancement mechanism.[223]

Le Goas *et al.* evaluated the effects of ionizing radiations on ligands by using AuNPs stabilized by thiol-ended polymer chains.[216] Characterization of the polymer corona before and after irradiation by γ rays at different doses revealed two degradation pathways of polymeric ligands: degrafting (proximal scissions) or partial shaving of the polymer corona (distal scissions) (**Figure 5C**). The authors hypothesized either a surface catalytic effect or the impact of hot electrons produced by plasmon excitation. X-ray irradiation of AuNPs was also reported to break DNA strands used as ligands[224] and to generate greater damage in proteins, compared to irradiation without NPs.[225] In the case of QDs, high-energy photons (both X-rays and γ rays) were shown to accelerate the photocatalytic oxidation of the thiol surface ligands.[226]

Several studies have also indirectly demonstrated the effect of irradiation on ligand fate, showing a lower production of secondary electrons upon X-ray and proton irradiation of radiosensitizing ligand-coated NPs compared to naked NPs.[227–229] Gilles *et al.* observed similar trends for the production of free radicals by irradiated PEG-coated AuNPs.[230] The authors hypothesized that ligands could trap the secondary electrons initially emitted or the free radicals later generated. Lower radiosensitizing efficiencies were indeed obtained in both experimental and simulation studies for ligand-coated NPs.[231,232] As we may expect an impact of these reactive species on the ligands during the process, these results tend to confirm that ionizing radiations can induce the degradation of ligands located on radiosensitizing NPs.

3.5.4. Effects of UV and visible light

Apart from high-energy photons, NP surfaces are also often exposed to UV and visible light, whether in their environment or for characterization purposes. Even with lower energy, this type of radiation can potentially affect the surface ligands of NPs. UV-induced oxidation was, for instance, already mentioned in the *Chemical degradation* section.[82] Another study by Borah *et al*. investigated the photostability of semiconductor metal-oxide NPs (TiO_2, ZnO, WO_3, and CuO) capped with oleylamine or alkyl thiol ligands.[233] Fast photodegradation of ligands was observed for multiple NP-ligand pairs, under both UV and white light.

The technique of laser desorption/ionization mass spectrometry (LDI-MS) is another example of light-induced ligand degradation. The mechanism consists of irradiating NPs with a laser, which energy is absorbed by the NP core, causing ionization and desorption of the surface ligands. The technique has been used with both AuNPs and IONPS to provide information on ligand composition (**Figure 5D**).[217,234]

The use of light as an environmental trigger for drug delivery has also been reported. For instance, Chen *et al.* designed a light-enabled reversible self-assembly and disassembly system based on AuNPs capped with photo-responsive polymer chains.[235] Irradiation with 365- and 254-nm UV light respectively induced photo-crosslinking and photocleavage of the polymer coating. This light-triggered self-assembly and disassembly process was shown to enable dye encapsulation and release.

All these studies reveal that external stimuli (light, magnetic field, ionizing radiations) intended to enhance the therapeutic effects of inorganic NPs may also impact the ligands located at their surface. Very few studies have directly addressed the subject, while others provide indirect proof of a degradation phenomenon. The translation of these effects to biological environments should be investigated in the future, as most experiments were performed in non-physiological conditions.

4. Ligand fate in biological media

In vivo, nanoparticles are immersed in complex media composed of cells, extracellular vesicles, proteins, lipids, ionic species, etc. In this environment, all the mechanisms mentioned in the previous sections may modulate ligand chemical structure, integrity, and surface density. Surface coatings can be displaced by proteins and lipids or degraded by enzymes or by chemical reactions related to pH or redox conditions found, for instance, in tumors' microenvironment or the cytosol of cells. As a consequence, ligand degradation could play a role in determining particle pharmacokinetics and efficacy *in vivo*.

The quantitative detection of surface ligand alteration *in vitro* and *in vivo* is not a trivial issue, as it relies on the ability to detect independently the different components of the particulate system and to follow their individual and collective fate in a complex biological matrix and/or in multiple organs. In such a complex environment, it is even more challenging to identify the mechanistic origins of the changes occurring at the surface of the particle. If the characterization technique allows it, particles and ligands (attached or free) are preferably quantified directly *in vivo* or *ex vivo* in the biological matrix. Alternatively, it is often necessary to extract biological samples containing particles and ligands and to separate them from other biological fluids and tissue components before analysis and quantification. This purification step must be quantitative, efficient, and should not affect the integrity of particle components to be analyzed.

Most studies focusing on ligand biological fate have used labeling strategies. Fluorescence labeling has some handling advantages, but the attachment of a fluorescent dye may greatly modify the physicochemical properties of either the particle core or the ligands,[236,237] and therefore influence the degradation of the particle. The use of particles with strong optical properties such as QDs or AuNPs can circumvent this problem by removing the necessity for core-specific labeling. Alternatively, radiolabeling is a technique with a marginal effect on physicochemical properties, usually stable, and allowing whole-body imaging and quantification. To track the particle core, labeling can be performed by the addition of iron isotopes in the case of IONPs[44,238,239] or by post-synthesis neutron activation of gold in the case of AuNPs.[45] The organic coating can also be modified, for instance, by incorporating ^{14}C in organic ligands[44,239] or by the addition of groups that chelate radioactive elements.[45,134,239] However, there is a limited number of laboratories able to perform such labeling on particles and their organic ligands, as well as to process and analyze radioactive samples.

When deciding on a labeling strategy, one should be able to detect intact particle systems as well as detached free ligands and partially degraded particles. In other words, one should be able to distinguish unambiguously and quantitatively the ligand signal from that of the particle core. This is usually done by colocalization of the two signals at the organ level. Detection modalities allowing direct correlation between core and ligand signals are scarce. Only Förster resonance energy transfer (FRET) and related techniques allow to study the particle coating stability *in vivo* and to determine if ligands are still associated with the core.[240] As the efficiency of the energy transfer from donor to acceptor is inversely proportional to the distance separating them, if the donor dye is attached to the core and the acceptor dye is bound to the surface ligand, the integrity of the NP system can be monitored.[240]

Finally, laser desorption/ionization mass spectrometry (LDI-MS) has been proposed to characterize the surface ligands of inorganic NPs such as AuNPs or QDs in complex environments.[28,234,241,242] As already mentioned in the section about external stimuli, LDI triggers the desorption and ionization of ligands, allowing a semi-quantitative determination of the monolayer composition by MS.[217,234] To our knowledge, LDI-MS is the only label-free technique able to evaluate the intracellular fate of ligands on inorganic particles.

Considering the mentioned technical difficulties for *in vivo* studies, the stability of surface ligands in biological environments has often been investigated using protein-containing media

or intracellular environments. So far, *in vivo* animal studies are very uncommon. **Table 2** gives an overview of all studies performed in these three different conditions.

4.1. Protein-containing media

When injected in biological fluids, particles are exposed to proteins that bind to their surface and form a protein corona. As already mentioned, enzymes are able to degrade some ligands.[111] Hence, a PC composed of enzymes could potentially cause/accelerate the degradation of surface ligands. The role of the PC on the degradation of ligands at the surface of NPs was directly demonstrated by Portilla *et al.*[243] The authors identified several enzymes, including 20% of hydrolases, in the PC of dextran-coated IONPs exposed to FBS. The degradation of different organic ligands was monitored by IR spectroscopy following 24h-exposure to 10% FBS. The presence of FBS in the incubation medium greatly accelerated the degradation of the coatings, especially dextran.

4.2. Intracellular environments

When exposed to *in vivo* conditions, NPs often undergo cell uptake and intracellular trafficking in endosomes and lysosomes. These intracellular vesicles expose endocytosed materials to enzymatic, pH, and redox conditions, which can greatly affect ligand stability and particle integrity. This can in turn impact the intracellular fate of particles, such as their degradation and endosomal escape, as well as their efficacy. For instance, the nature of the ligands, and therefore their stability, was shown to be the determining factor for the endosomal degradation rate of IONPs.[244] Lunov *et al.* also reported the intracellular degradation of a fluorescently labeled carboxydextran coating of IONPs.[106] Internalization of carboxydextran-IONPs in macrophages induced a decrease in the intracellular fluorescence signal from the ligand over time, while iron contents in cellular vesicles remained unchanged. This result, along with DLS showing a decreased diameter from cells-recovered IONPs, indicated degradation of the carboxydextran coating in macrophage vesicles. Subcellular localization by fluorescence microscopy showed that IONPs were confined to lysosomes containing α-glucosidase (an enzyme for which dextran is a substrate), suggesting that coating loss was mainly due to enzymatic degradation.[106]

Likewise, the intracellular fate of inorganic nanoparticles composed of an Eu- and Bi-doped gadolinium core and an organic coating of polyacrylic acid (PAA) was explored in cultured

cells.[245] Cores were detected by elemental analysis while the surface coating was labeled by fluorescein amine (FA) and detected by fluorescence. NP cores were shown to be remodeled from cubic to rounded shapes by the acidic conditions in the late endosome/lysosome. Additionally, cytometry data suggested that FA-labeled PAA coatings were enzymatically degraded inside endosomal/lysosomal compartments and that polymer fragments were exocytosed at a faster rate than cores. However, the results were strictly qualitative as the authors were unable to quantify these effects.[245]

Fluorophore quenching was alternatively proposed to assess ligand stability during cell uptake and intracellular processing of QDs.[246] Red fluorescent QDs were surface-modified with a polymer coating labeled with 5-carboxyfluorescein, which fluorescence emission was quenched by proximity to the QD core. The authors concluded that polymer ligands dissociated from the core in lysosomes as the polymer-associated fluorescence was emerging.[246] Similarly, Sée *et al.* studied the fate of AuNPs conjugated with fluorescent peptides after cell uptake.[113] Initially quenched by the NP core, the intracellular fluorescence increased over time, indicating the release of the fluorophore. Complementary experiments performed with various inhibitors suggested that the peptides were degraded inside the endosomes by enzymes such as the protease cathepsin L. The authors estimated that more than a third of the human proteome could be cleaved by this enzyme, which could be an issue for active targeting strategies.

The stability of QDs organic coating during intracellular trafficking was also studied with a triple-labeled NP system.[247] To better understand the fate of NPs, the authors designed QDs with a fluorescently-labeled polymer coating (dodecylamine-modified PMA) and an adsorbed (or covalently crosslinked) layer of fluorescently-labeled HSA. Upon incubation with cells, both adsorbed and crosslinked HSA were transported by NPs into cells and retained inside endosomes and lysosomes for a longer time compared to free HSA. The polymer coating was degraded intracellularly, and QDs were found to be exocytosed faster than polymer fragments. Crosslinking of the polymer coating was also shown to enhance the stability of the assembly. The authors concluded that polymer degradation was slower than the exchange/desorption of adsorbed HSA.[247]

Besides hydrophilic polymer ligands, targeting antibodies immobilized on AuNPs can also be detached during cell internalization.[135] The authors used the luminescence properties of 5 nm AuNPs to study the intracellular trafficking and fate of AuNPs functionalized with both 5kDa

PEG ligands and fluorescently-labeled epidermal growth factor receptor (EGFR)-targeting antibody. Both PEG and antibody ligands were attached via gold-thiol chemistry. Inside the cells, the coating detached from the core resulting in the formation of particle clusters with a strong luminescence signal inside the endosomes, as detected by two-photon microscopy. Additionally, the authors revealed a spatial separation of gold cores and fluorescent-labeled antibody coating, confirming the detachment of the targeting ligand from the core during vesicular transport. *In vitro* results suggested the possible involvement of ligand exchange with intracellular GSH for the release of antibodies from the gold cores.[135] Such a mechanism could also be involved in the observed NP aggregation, as ligand exchange decreases PEG surface density and may trigger colloidal instability as a result. Noteworthy, excess GSH could also reduce disulfide bonds maintaining the tertiary structure of the antibody.

The involvement of the intracellular redox state on ligand stability was also demonstrated by Hong *et al*.[131] The thiolated dye attached to AuNPs was shown to be released from the NP surface after cell internalization. Moreover, the dye release seemed to be dependent on the intracellular concentration of GSH, suggesting ligand exchange between thiolated entities.

The role of enzymatic and redox states was further investigated by Rosi *et al*.[248] In their study, mono- or tetrathiol antisense oligonucleotides were attached to the AuNP surface. Oligonucleotides were labeled with both Cy3 dye near the anchor and Cy5.5 dye attached to the end of the strand. Fluorescence of the two dyes was monitored upon NP cell uptake, as fluorescence intensity was dependent on ligand release from the quenching gold core. Intracellular nucleases were found responsible for Cy5.5 increased emission. On the other hand, Cy3 intensity remained low, even at high GSH concentration, suggesting high resistance of the system to thiol ligand exchange for both mono- and tetrathiol anchoring groups.

Since the fluorescence lifetime of luminescent NPs depends on their surface coating and structural integrity, it was proposed to monitor the ligand stability of QDs and AuNPs after cell uptake.[249] Compared to fluorescence intensity, lifetime is not affected by exocytosis or cell division. The observed changes in QD fluorescence lifetime were attributed to ligand exchange with biomolecules and subsequent acidic degradation of the cores in lysosomes. Different behaviors were reported for different ligands, thus demonstrating variations in the ability of ligands to protect the cores. Of note, AuNPs coated with the same ligands were much more stable than QDs, underscoring the importance of the strength of core-ligand attachment for

intracellular stability. This aspect was also highlighted in a study comparing regular AuNPs with AuNPs covered by a thin layer of platinum (Au@Pt NPs).[173] Single-stranded DNA dual-modified with thiol and fluorophore (Cy3) were attached to both types of NPs. Both nanosystems resisted well degradation by DNAse in physiological concentrations, while exposure to biothiols (GSH and cysteine) correlated with the release of the DNA strands from AuNPs but not from Au@Pt NPs. Similar behaviors were obtained intracellularly. Only the addition of a thiol scavenger prevented DNA release from AuNPs, which confirmed that biothiols were responsible for the release. Pt-S bond was found to be much more resistant than Au-S to exchange with biothiols.

To date, LDI-MS is the only label-free technique able to evaluate the intracellular fate of ligands on inorganic particles. Initially developed to characterize the thiolated monolayer of AuNPs post-synthesis,[234] the same approach was successfully applied to follow the intracellular stability of QD thiolated monolayers in cells.[241] A combination of LDI-MS and inductively coupled plasma mass spectrometry (ICP-MS) enabled a measurement of the ligands released from cell-uptaken AuNPs, and thus an evaluation of their intracellular stability.[242]

These studies demonstrate that endocytosed NPs can be transformed during their journey across the cell vesicular system. This implies that in case of subsequent exocytosis, NPs could be found again in circulation with altered properties, which could lead to changes in pharmacokinetics and undesired biopharmaceutical outcomes. Such a phenomenon can also have a major impact in the context of cancer treatment, as Sindhwani *et al.* recently showed that the vast majority of NPs enter the tumoral environment via active transendothelial trafficking rather than via passive extravasation through tumor vessel pores, as previously thought.[250] If NP uptake by endothelial cells leads to a certain level of ligand degradation before their delivery to the tumor microenvironment, it could have deleterious effects on the NP efficacy, especially on tumor-targeting capabilities.

4.3. *In vivo* studies

Ferumoxtran-10 is a representative example of stability issues in biological media faced by inorganic NPs modified with organic ligands. Ferumoxtran is an NMR contrast agent with a diameter of 30 nm, composed of an iron oxide core coated with adsorbed low molecular weight dextran.[251] The blood half-life of this NP varies from 1 to 24-36 hours and is dependent on both the surface coating and the size of NPs. Once taken up by macrophage cells, the IONPs

are degraded in the lysosomes. The dextran coatings are enzymatically degraded by intracellular dextranases, as demonstrated by Lunov *et al.*,[106] and their degradations products are excreted in the urine. The toxicity issues of IONPs (many products have been withdrawn from the market)[252] are related to the release of ionic forms of Fe causing oxidative damage. Improved coating stability *in vivo* could help prevent the exposition of catalytic surface sites, the release of Fe ions, and oxidative damage.[251] As the example of IONPs shows, there is a direct relationship between performance and ligand stability.

However, as mentioned above, *in vivo* investigation of ligand stability is associated with several technical issues, hence the low number of *in vivo* studies. Kreyling *et al.* designed radiolabeled 5 nm gold cores (^{198}Au) functionalized with a ^{111}In-labeled polymer coating.[45] Upon intravenous injection into rats, the biodistribution of ^{198}Au and ^{111}In revealed partial stripping of the polymer coating. Indeed, gold cores appeared to accumulate mostly in the liver while part of the ^{111}In signal displayed a biodistribution similar to intravenously injected chelated ^{111}In alone. Complementary *in vitro* experiments suggested that degradation of the polymer shell was caused by proteolytic enzymes in the liver.

Silva *et al.* described similar experiments with AuNPs surface-modified with an organic coating attached to the NP core by Au-S bonds and crosslinked with disulfide bonds.[134] An interesting feature of this coating is its ability to complex ^{99m}Tc. *In vivo* experiments in mice demonstrated that the release of ^{99m}Tc was due to the coating detachment from the NP. *In vitro* data suggested that GSH level in mice blood could be responsible for coating shedding through ligand exchange and/or cleavage of disulfide bonds.

Wang *et al.* also used radiolabeling to investigate the ligand stability of IONPs stabilized by oleic acid and phospholipids.[239] Cores were radiolabeled with ^{59}Fe, while oleic acid and phospholipid surface ligands were respectively labeled with ^{14}C and chelated with ^{111}In. Biodistribution experiments in mice showed that ^{111}In is preferentially localized in organs rich in phagocytic cells such as the liver, spleen, and bones. Compared to ^{111}In, higher levels of ^{59}Fe were reported in the liver and spleen, suggesting some core-phospholipid shell dissociation. Very low levels of ^{14}C were reported in these organs, evidencing an extensive dissociation of the oleic acid component from the iron oxide core. The *in vivo* instability of oleic acid coating on IONPs labeled with ^{59}Fe had been previously established by Freund *et al.*[44]

Elci *et al.* proposed to follow and correlate the core and shell of NPs in organs by combining two techniques initially developed to characterize ligands post-synthesis or after cell uptake.[234,241,242] Laser ablation inductively-coupled plasma mass spectrometry (LA-ICP-MS) imaging was used to detect the gold NP core, while LDI-MS imaging was used to detect the distribution of ligands, including those still bound to the NP core.[28] AuNPs functionalized with monolayers of different surface ligands were injected in mice. After collection of organs and cryo-sectioning, imaging was performed and analyzed for core and coating signals colocalization. It was determined that the chemical stability of the particle coating was significantly different in the liver and spleen. Complete degradation of the coating was observed in the liver after 24h, where only the signal from the NP core was recovered. This is in contrast with *in vitro* assays performed with hepatocytes, which showed better stability of the NP coating. The difference may originate from the more complex environment encountered by NPs *in vivo*, which includes macrophages and liver sinusoidal endothelial cells as well as flow. In the spleen, ligands were more stable but showed marked differences in stability depending on the location within the organ. This study underlines the importance of *in vivo* stability studies, as *in vitro* assays were found to poorly predict *in vivo* results.[28] Even though the spatial resolution of the imaging technique allowed to correlate the core and ligand signals at the sub-organ level, it is still unclear if ligands remained associated with the core.

In a similar approach, AuNPs coated with PEG were intravenously injected in rats and mice.[253] After organ collection, cryosections of the liver, spleen, and kidney were examined by synchrotron X-ray fluorescence (XRF) and synchrotron Fourier-transform infrared spectroscopy (FTIR) to image the gold core and the PEG ligands, respectively. The authors observed that gold (in rats) and PEG (in mice) presented similar distribution patterns in sub-organ regions, suggesting stability of PEGylation on AuNPs. However, it is worth mentioning that the experiments were conducted on two different species (XRF on rats and FTIR on mice) and that the resolution of the imaging modalities could once again not entirely confirm PEG attachment to the gold cores.

Finally, an example illustrating the potential of FRET to investigate ligand stability *in vivo* was given by Yang *et al.*[254] The stability of QDs coated with polymer ligands complexed with Cy3-labeled human serum albumin (HSA) was followed *in vitro*, *in vivo*, and *ex vivo*. The NP was used as a FRET sensor as the HSA-associated Cy3 signal was emitted upon excitation of QDs at a specific wavelength, allowing to report the association of the protein with the QDs. *In vivo*

imaging study was conducted in human breast tumor-carrying mice. QDs were injected via the tail vein, and FRET imaging was performed on live animal. Good stability of the nanosystems was demonstrated. This study illustrates that FRET can be used to monitor ligand stability *in vivo*.

As revealed in this section, *in vivo* monitoring of ligand stability is currently under-investigated, partly because of technical issues, such as the isolation of particle components from the biological milieu, the need to tag each component, and the difficulty to distinguish between intact and degraded objects. This last challenge could be solved by implementing techniques such as FRET, yet having in mind the inherent limitation of fluorescence signal quantification in tissues due to limited signal penetration depth, quenching, and limited resolution of fluorescence imaging.[240]

Of note, almost all the *in vivo* studies reported here demonstrated ligand instability, but few of them identified the mechanisms involved, which were always inferred from *in vitro* results. One additional limitation is that these studies tested only one mechanism of degradation out of the few possible ones, which mitigates the significance of the conclusions. Indeed, several mechanisms are expected to be simultaneously at play *in vivo*.

Table 2. Ligand fate in biological media: *in vivo*-simulated conditions, intracellular, and *in vivo* measurements

Core	Ligands	Detection technique	Conditions	Outcomes	Hypothesized mechanism of degradation	Reference
Protein-containing media						
IONPs	PMA	Ligands: fluorescence labeling	Incubation with different enzymes and enzyme mixtures	Effect of enzymes on ligand stability	Enzymatic degradation	[111]
IONPs	Various ligands	FTIR analysis	Incubation in FBS	Ligand degradation in FBS for various ligands	Enzymatic degradation	[243]
Intracellular environments						
IONPs	Lipids, dextran, carboxydextran, citrate	Core: Colorimetric detection of released Fe^{3+}	Cell uptake (C17.2 cells and PC-2 cells)	Role of ligands on the intracellular core stability	Unidentified	[244]
IONPs	Carboxydextran	Ligands: fluorescence labeling with Oyster550 Core: Fe spectroscopic dosage	Cell uptake (macrophages)	Enzymatic degradation of ligands in macrophage vesicles (lysosomes)	Enzymatic degradation	[106]
Rare-earth NPs	Polyacrylic acid (PAA)	Ligands: fluorescence labeling with fluorescein amine	Cell uptake (HeLa cells)	Enzymatic degradation of ligands in endosome/lysosomal vesicles	Enzymatic degradation	[245]
QDs	PEG	Ligands: fluorescence labeling with 5-carboxyfluorescein (signal quenched when attached to QD core)	Cell uptake (PC-3 cells)	Dissociation of ligands in lysosomes	Unidentified	[246]
AuNPs	Peptides	Ligands: fluorescence labeling with fluorescein (signal quenched when attached to Au core)	Cell uptake (HeLa cells)	Enzymatic degradation of ligands in endosome vesicles	Enzymatic degradation	[113]
QDs	PMA + adsorbed or covalently linked HSA	Polymer: fluorescence labeling with ATTO488 HSA: fluorescence labeling with Cy7	Cell uptake (HeLa cells)	Enzymatic degradation and exocytosis of polymer ligands Rapid exchange and desorption of HSA	Enzymatic degradation	[247]

AuNPs	PEG and EGFR-targeting antibodies (dithiol linker)	Ligand: fluorescence labeling with AF647 Two-photon microscopy and FLIM were used	Cell uptake (A431 cells)	Intracellular detachment of ligands leading to core clusters	Ligand exchange with biothiols + Enzymatic degradation	[135]
QDs	Various thiolated ligands	Ligands: LDI-MS on cell extract Core: ICP-MS	Cell extract after uptake (HeLa cells)	Semi-quantitative determination of ligand composition after cell uptake	Ligand exchange with GSH	[241]
AuNPs	Various thiolated ligands	Ligands: LDI-MS on cell extract Core: ICP-MS	Cell extract after uptake (HeLa cells)	Semi-quantitative determination of ligand composition after cell uptake	Ligand exchange with GSH	[242]
QDs & gold nanoclusters	Thiolated ligands (covalent binding) and PEG-amine (hydrophobic interactions)	Measure of the fluorescence lifetime of cores as an indicator of ligand stability	Cell uptake (HeLa cells)	Semi-quantitative determination of ligand stability after cell uptake	Ligand exchange with biothiols	[249]
In vivo studies						
AuNPs	Amphiphilic polymer: poly(isobutylene-alt-maleic anhydride)-graft-dodecyl	Ligands: radioactive labeling with ^{111}In Core: radioactive labeling with ^{198}Au	*In vivo* rat experiments (i.v. injection)	Core accumulation in the liver Excretion of polymer ligands by kidney	Enzymatic degradation	[45]
AuNPs	Thiolated DTPA derivative	Ligands: radioactive labeling with ^{99m}Tc complexed in the crosslinked shell	*In vivo* mouse experiments (i.v. injection)	GSH-promoted ligand shedding followed by ^{99m}Tc release	Ligand exchange with biothiols or S-S bond cleavage	[134]
AuNPs	Different ligands composed of a mono- or dithiol anchoring group, a hydrophobic alkane segment, a tetra(ethylene glycol) segment, and a variable head group	Ligand: LDI-MS Core: LA-ICP-MS	*In vivo* mouse experiments: (i.v. injection and *ex vivo* imaging of liver and spleen)	Complete degradation of ligands in the liver Differences in ligand stability in different locations of the spleen	Ligand exchange with biothiols	[28]
IONPs	Oleic acid and phospholipids	Oleic acid: radioactive labeling with ^{14}C Phospholipids: radioactive labeling with chelated ^{111}In Core: radioactive labeling with ^{59}Fe	*In vivo* mouse experiments (i.v. injection)	Partial dissociation of phospholipids in liver and spleen Complete stripping of oleic acid from the core	Unidentified	[239]

IONPs	Oleic acid	Ligand: radioactive labeling with ^{14}C Core: radioactive labeling with ^{59}Fe	*In vivo* mouse experiments (i.v. injection)	Complete stripping of oleic acid from the core	Unidentified	[44]
AuNPs	PEG	Ligand: synchrotron FTIR Core: synchrotron X-ray fluorescence (XRF)	*In vivo* rat and mouse experiments (i.v. injection and *ex vivo* imaging of liver, spleen, and kidney)	Sub-organ colocalization of ligand and core signals	NA (stable ligands)	[253]
QDs	(Poly(diethylenetriamine-dihydrolipoic acid-L-glutamate) complexed with HSA	HSA: fluorescence labeling with Cy3 (FRET acceptor) Core: 525 nm emitting QDs (FRET donor)	*In vitro* (HeLa cells) and *in vivo* mouse experiments (i.v. injection)	Stable nanosystems	NA (stable ligands)	[254]

5. Conclusion and perspectives

In this review, multiple mechanisms are shown to alter the surface ligands of inorganic NPs intended for biomedical applications, both during their shelf-life and upon their intended use in biological environments. Considering that ligands govern the interactions of NPs with their environment and that they are frequently used to graft targeting agents or drugs, their degradation may greatly impact the NP properties and efficacy. Characterization of ligand degradation phenomena is therefore key to improving our understanding of the biological behavior of nanomedicines.

The relatively small number of studies focusing on ligand stability emphasizes the critical need to develop this field of research, to answer both fundamental questions and considerations for clinical applications. The nature and strength of ligand-NP bonds are, for instance, poorly understood, and recent reports point towards the key role of the local chemical environment.[255–257] Storage stability studies are also lacking, although they are necessary for clinical translation. Reports of post-synthesis spontaneous mechanisms further highlight the need to carry out such studies, with specific attention to the surface coating. Finally, investigations performed under conditions more representative of biological systems are required. Indeed, as already mentioned, intracellular and *in vivo* studies are scarce. Moreover, some degradation pathways, such as chemical ones and the ones occurring under external stimuli, have only been reported in fundamental studies or in the context of other research fields. As a result, direct application of these results to nanomedicine is limited, and future work should strive to tackle these questions.

We have already pointed out the underlying issue of the difficult characterization of surface ligands *in situ*, especially *in vivo*. Innovative techniques suitable for such *in situ* analysis are thus needed and should become a common goal for the nanomedicine community. The development of refined *in vitro* models with improved representativeness of biological systems is also essential, as they constitute an easier and viable alternative to *in vivo* studies in the short term. The expanding skills in microfluidics and 3D cell culture have, for instance, allowed to develop organs-on-chips that better mimic the complexity and dynamic features of biological environments and that are more compatible with classical characterization techniques.[258]

The ligand instability evidenced by the few *in vivo* studies reported so far also highlights the inherent risks of complex nanosystems combining multiple functionalities. Such designs are already challenging to properly characterize post-synthesis, and their potential degradation into multiple individual components further complicates the monitoring of their fate *in vivo*. The multiplication of components also increases the likelihood of instability and hinders the understanding of NP behavior. Ultimately, this compromises the efficacy of NPs and hampers their clinical translation. Consequently, it is legitimate to question the trend towards complex applications we have witnessed in nanomedicine literature this past decade. The relatively low number of nanomedicines on the market further advocates for more simplicity in NP design.[259]

The investigation of ligand (in)stability finally raises the question of the consequences of such instability. We already mentioned the reduced colloidal stability, the altered properties of the NP, the degradation of a drug, and the loss of targeting effects, all of which may modify the NP pharmacokinetics and efficacy. Ligand degradation may also create some heterogeneity in the NP population, which hampers the prediction of their behavior.[260] Furthermore, toxicity may arise from the degraded products. For instance, ligand degradation was shown to increase the toxicity of IONPs due to surface reconstruction of the cores,[261] while AuNRs covered with unstable ligands disrupted the cell membrane integrity, which generated cytotoxicity and inflammatory responses.[262] However, instability can also be seen as a positive feature, promoting biodegradation and elimination. The persistence of nanomaterials *in vivo* may indeed cause problems in the long term.[263] Overall, we believe that a better understanding of the ligand degradation phenomena will be necessary to rationally design NPs with adequate and tunable (in)stability. This improved knowledge will eventually favor the development of clinically sound approaches.

Acknowledgments

MLG was supported by an FRQS postdoctoral research scholarship. This research was undertaken thanks, in part, to funding from the Canada First Research Excellence Fund through the Trans-MedTech Institute (MLG postdoctoral fellowship, JS doctoral scholarship) and from the Natural Sciences and Engineering Research Council of Canada via the NSERCCREATE PrEEmiuM program (JS doctoral scholarship). JS thanks the faculty of pharmacy (UdeM) for

the PhD scholarship. XB acknowledges the support from the CRC program, from FRQS under the umbrella of ERA-NET EuroNanoMed (GA N°723770) of the EU Horizon 2020 Research and Innovation Program, from NSERC, and from FRQNT.

Received: ((will be filled in by the editorial staff))
Revised: ((will be filled in by the editorial staff))
Published online: ((will be filled in by the editorial staff))

References

[1] M. R. K. Ali, Y. Wu, M. A. El-Sayed, *J. Phys. Chem. C* **2019**, *123*, 15375.

[2] S. Her, D. A. Jaffray, C. Allen, *Advanced Drug Delivery Reviews* **2017**, *109*, 84.

[3] C. Blanco-Andujar, A. Walter, G. Cotin, C. Bordeianu, D. Mertz, D. Felder-Flesch, S. Begin-Colin, *Nanomedicine* **2016**, *11*, 1889.

[4] A. Heuer-Jungemann, N. Feliu, I. Bakaimi, M. Hamaly, A. Alkilany, I. Chakraborty, A. Masood, M. F. Casula, A. Kostopoulou, E. Oh, K. Susumu, M. H. Stewart, I. L. Medintz, E. Stratakis, W. J. Parak, A. G. Kanaras, *Chem. Rev.* **2019**, *119*, 4819.

[5] J. J. Calvin, A. S. Brewer, A. P. Alivisatos, *Nat Synth* **2022**, *1*, 127.

[6] A. Albanese, W. C. W. Chan, *ACS Nano* **2011**, *5*, 5478.

[7] B. Halamoda-Kenzaoui, M. Ceridono, P. Urbán, A. Bogni, J. Ponti, S. Gioria, A. Kinsner-Ovaskainen, *Journal of Nanobiotechnology* **2017**, *15*, 48.

[8] T. L. Moore, A.-S. Schreurs, R. A. Morrison, E. K. Jelen, J. Loo, R. K. Globus, F. Alexis, *Journal of Nanomedicine & Nanotechnology* **2014**, *05*, DOI 10.4172/2157-7439.1000237.

[9] D. Kwon, J. Park, J. Park, S. Y. Choi, T. H. Yoon, *Int J Nanomedicine* **2014**, *9*, 57.

[10] F. Schulz, G. T. Dahl, S. Besztejan, M. A. Schroer, F. Lehmkühler, G. Grübel, T. Vossmeyer, H. Lange, *Langmuir* **2016**, *32*, 7897.

[11] H. T. T. Duong, Y. Chen, S. Abdulkader Tawfik, S. Wen, M. Parviz, O. Shimoni, D. Jin, *RSC Advances* **2018**, *8*, 4842.

[12] P. Cao, L. Tong, Y. Hou, G. Zhao, G. Guerin, M. A. Winnik, M. Nitz, *Langmuir* **2012**, *28*, 12861.

[13] E. Oh, K. Susumu, A. J. Mäkinen, J. R. Deschamps, A. L. Huston, I. L. Medintz, *J. Phys. Chem. C* **2013**, *117*, 18947.

[14] J. Liu, D. A. Sonshine, S. Shervani, R. H. Hurt, *ACS Nano* **2010**, *4*, 6903.

[15] J. Kolosnjaj-Tabi, Y. Javed, L. Lartigue, J. Volatron, D. Elgrabli, I. Marangon, G. Pugliese, B. Caron, A. Figuerola, N. Luciani, T. Pellegrino, D. Alloyeau, F. Gazeau, *ACS Nano* **2015**, *9*, 7925.

[16] I. V. Zelepukin, A. V. Yaremenko, I. N. Ivanov, M. V. Yuryev, V. R. Cherkasov, S. M. Deyev, P. I. Nikitin, M. P. Nikitin, *ACS Nano* **2021**, DOI 10.1021/acsnano.1c00687.

[17] S. E. Lehman, I. A. Mudunkotuwa, V. H. Grassian, S. C. Larsen, *Langmuir* **2016**, *32*, 731.

[18] B. D. Johnston, W. G. Kreyling, C. Pfeiffer, M. Schäffler, H. Sarioglu, S. Ristig, S. Hirn, N. Haberl, S. Thalhammer, S. M. Hauck, M. Semmler-Behnke, M. Epple, J. Hühn, P. Del Pino, W. J. Parak, *Advanced Functional Materials* **2017**, *27*, 1701956.

[19] F. Simonelli, G. Rossi, L. Monticelli, *J. Phys. Chem. B* **2019**, *123*, 1764.

[20] Z. Zhang, K. Van Steendam, S. Maji, L. Balcaen, Y. Anoshkina, Q. Zhang, G. Vanluchene, R. De Rycke, F. Van Haecke, D. Deforce, R. Hoogenboom, B. G. De Geest, *Adv. Funct. Mater.* **2015**, *25*, 3433.

[21] L. Gong, Y. Chen, K. He, J. Liu, *ACS Nano* **2019**, DOI 10.1021/acsnano.8b08103.

[22] M. Le Goas, T. Roussel, M. Kalbazova, D. Carrière, E. Barruet, V. Geertsen, G. Fadda, F. Testard, G. Carrot, J.-P. Renault, *Journal of Materials Chemistry B* **2020**, *8*, 6438.

[23] M. Li, S. Jiang, J. Simon, D. Paßlick, M.-L. Frey, M. Wagner, V. Mailänder, D. Crespy, K. Landfester, *Nano Lett.* **2021**, DOI 10.1021/acs.nanolett.0c03756.

[24] H. Sun, C. Jiang, L. Wu, X. Bai, S. Zhai, *Frontiers in Bioengineering and Biotechnology* **2019**, *7*, 414.

[25] L. Tomasetti, R. Liebl, D. S. Wastl, M. Breunig, *European Journal of Pharmaceutics and Biopharmaceutics* **2016**, *108*, 145.

[26] M. Le Goas, F. Testard, O. Taché, N. Debou, B. Cambien, G. Carrot, J.-P. Renault, *Langmuir* **2020**, *36*, 10460.

[27] Y. Tang, S. Han, H. Liu, X. Chen, L. Huang, X. Li, J. Zhang, *Biomaterials* **2013**, *34*, 8741.

[28] S. G. Elci, G. Yesilbag Tonga, B. Yan, S. T. Kim, C. S. Kim, Y. Jiang, K. Saha, D. F. Moyano, A. L. M. Marsico, V. M. Rotello, R. W. Vachet, *ACS Nano* **2017**, *11*, 7424.

[29] N. Bertrand, P. Grenier, M. Mahmoudi, E. M. Lima, E. A. Appel, F. Dormont, J.-M. Lim, R. Karnik, R. Langer, O. C. Farokhzad, *Nat Commun* **2017**, *8*, 777.

[30] G. Stepien, M. Moros, M. Pérez-Hernández, M. Monge, L. Gutiérrez, R. M. Fratila, M. de las Heras, S. Menao Guillén, J. J. Puente Lanzarote, C. Solans, J. Pardo, J. M. de la Fuente, *ACS Appl. Mater. Interfaces* **2018**, *10*, 4548.

[31] X. Li, B. Wang, S. Zhou, W. Chen, H. Chen, S. Liang, L. Zheng, H. Yu, R. Chu, M. Wang, Z. Chai, W. Feng, *Journal of Nanobiotechnology* **2020**, *18*, 45.

[32] J.-M. Montenegro, V. Grazu, A. Sukhanova, S. Agarwal, J. M. de la Fuente, I. Nabiev, A. Greiner, W. J. Parak, *Advanced Drug Delivery Reviews* **2013**, *65*, 677.

[33] D. C. Luther, R. Huang, T. Jeon, X. Zhang, Y.-W. Lee, H. Nagaraj, V. M. Rotello, *Advanced Drug Delivery Reviews* **2020**, *156*, 188.

[34] Y.-L. Luo, Y.-S. Shiao, Y.-F. Huang, *ACS Nano* **2011**, *5*, 7796.

[35] P. D. Pietro, L. Zaccaro, D. Comegna, A. D. Gatto, M. Saviano, R. Snyders, D. Cossement, C. Satriano, E. Rizzarelli, *RSC Advances* **2016**, *6*, 112381.

[36] Q. Dai, S. Wilhelm, D. Ding, A. M. Syed, S. Sindhwani, Y. Zhang, Y. Y. Chen, P. MacMillan, W. C. W. Chan, *ACS Nano* **2018**, *12*, 8423.

[37] J. Yin, D. Yao, G. Yin, Z. Huang, X. Pu, *ACS Appl. Mater. Interfaces* **2019**, *11*, 41038.

[38] M. Ruzycka-Ayoush, P. Kowalik, A. Kowalczyk, P. Bujak, A. M. Nowicka, M. Wojewodzka, M. Kruszewski, I. P. Grudzinski, *Cancer Nano* **2021**, *12*, 8.

[39] L. Digiacomo, S. Palchetti, F. Giulimondi, D. Pozzi, R. Z. Chiozzi, A. Laura Capriotti, A. Laganà, G. Caracciolo, *Lab on a Chip* **2019**, *19*, 2557.

[40] D. Sanchez-Guzman, G. Giraudon--Colas, L. Marichal, Y. Boulard, F. Wien, J. Degrouard, A. Baeza-Squiban, S. Pin, J. P. Renault, S. Devineau, *ACS Nano* **2020**, *14*, 9073.

[41] X. Tan, K. Welsher, *Angewandte Chemie International Edition* **2021**, DOI 10.1002/anie.202105741.

[42] J.-M. Rabanel, P. Hildgen, X. Banquy, *Journal of Controlled Release* **2014**, *185*, 71.

[43] E. Colangelo, J. Comenge, D. Paramelle, M. Volk, Q. Chen, R. Lévy, *Bioconjugate Chem.* **2017**, *28*, 11.

[44] B. Freund, U. I. Tromsdorf, O. T. Bruns, M. Heine, A. Giemsa, A. Bartelt, S. C. Salmen, N. Raabe, J. Heeren, H. Ittrich, R. Reimer, H. Hohenberg, U. Schumacher, H. Weller, P. Nielsen, *ACS Nano* **2012**, *6*, 7318.

[45] W. G. Kreyling, A. M. Abdelmonem, Z. Ali, F. Alves, M. Geiser, N. Haberl, R. Hartmann, S. Hirn, D. J. de Aberasturi, K. Kantner, G. Khadem-Saba, J.-M. Montenegro, J. Rejman, T. Rojo, I. R. de Larramendi, R. Ufartes, A. Wenk, W. J. Parak, *Nature Nanotechnology* **2015**, *10*, 619.

[46] N. Feliu, D. Docter, M. Heine, P. del Pino, S. Ashraf, J. Kolosnjaj-Tabi, P. Macchiarini, P. Nielsen, D. Alloyeau, F. Gazeau, R. H. Stauber, W. J. Parak, *Chemical Society Reviews* **2016**, *45*, 2440.

[47] S. Roy, Z. Liu, X. Sun, M. Gharib, H. Yan, Y. Huang, S. Megahed, M. Schnabel, D. Zhu, N. Feliu, I. Chakraborty, C. Sanchez-Cano, A. M. Alkilany, W. J. Parak, *Bioconjugate Chem.* **2019**, *30*, 2751.

[48] M. J. Hostetler, A. C. Templeton, R. W. Murray, *Langmuir* **1999**, *15*, 3782.

[49] J. Conde, J. T. Dias, V. Grazú, M. Moros, P. V. Baptista, J. M. de la Fuente, *Frontiers in Chemistry* **2014**, *2*, 48.

[50] C. Cruje, D. B. Chithrani, *Reviews in Nanoscience and Nanotechnology* **2014**, *3*, 20.

[51] A. Caragheorgheopol, V. Chechik, *Physical Chemistry Chemical Physics* **2008**, *10*, 5029.

[52] C. D. Walkey, J. B. Olsen, H. Guo, A. Emili, W. C. W. Chan, *J. Am. Chem. Soc.* **2012**, *134*, 2139.

[53] M. Uz, V. Bulmus, S. Alsoy Altinkaya, *Langmuir* **2016**, *32*, 5997.

[54] A. M. Jackson, J. W. Myerson, F. Stellacci, *Nature Mater* **2004**, *3*, 330.

[55] R. M. Choueiri, E. Galati, H. Thérien-Aubin, A. Klinkova, E. M. Larin, A. Querejeta-Fernández, L. Han, H. L. Xin, O. Gang, E. B. Zhulina, M. Rubinstein, E. Kumacheva, *Nature* **2016**, *538*, 79.

[56] S. Carregal-Romero, S. Plaza-García, R. Piñol, J. Murillo, J. Ruiz-Cabello, D. Padro, A. Millán, P. Ramos-Cabrer, *Biosensors* **2018**, *8*, 127.

[57] V. Chechik, *J. Am. Chem. Soc.* **2004**, *126*, 7780.

[58] Y. Ma, V. Chechik, *Langmuir* **2011**, *27*, 14432.

[59] D.-B. Grys, B. de Nijs, A. R. Salmon, J. Huang, W. Wang, W.-H. Chen, O. A. Scherman, J. J. Baumberg, *ACS Nano* **2020**, *14*, 8689.

[60] M. Horáček, D. J. Engels, P. Zijlstra, *Nanoscale* **2020**, *12*, 4128.

[61] J. Aldana, N. Lavelle, Y. Wang, X. Peng, *J. Am. Chem. Soc.* **2005**, *127*, 2496.

[62] G. Kalyuzhny, R. W. Murray, *J Phys Chem B* **2005**, *109*, 7012.

[63] J. Lacava, A. Weber, T. Kraus, *Particle & Particle Systems Characterization* **2015**, *32*, 458.

[64] I. F. Tannock, D. Rotin, *Cancer Res* **1989**, *49*, 4373.

[65] S. Mura, J. Nicolas, P. Couvreur, *Nature Mater* **2013**, *12*, 991.

[66] A. Kumari, S. K. Yadav, S. C. Yadav, *Colloids and Surfaces B: Biointerfaces* **2010**, *75*, 1.

[67] C. Lemarchand, R. Gref, P. Couvreur, *European Journal of Pharmaceutics and Biopharmaceutics* **2004**, *58*, 327.

[68] M. Nabavinia, J. Beltran-Huarac, *ACS Appl. Bio Mater.* **2020**, *3*, 8172.

[69] O. S. Muddineti, B. Ghosh, S. Biswas, *International Journal of Pharmaceutics* **2015**, *484*, 252.

[70] A. M. Basedow, K. H. Ebert, H. J. Ederer, *Macromolecules* **1978**, *11*, 774.

[71] J. A. Jennings, in *Chitosan Based Biomaterials: Fundamentals, Volume 1* (Eds.: J.A. Jennings, J.D. Bumgardner), Woodhead Publishing, **2017**, pp. 159–182.

[72] J. Hradil, A. Pisarev, M. Babič, D. Horák, *China Particuology* **2007**, *5*, 162.

[73] P. van de Wetering, N. J. Zuidam, M. J. van Steenbergen, O. A. G. J. van der Houwen, W. J. M. Underberg, W. E. Hennink, *Macromolecules* **1998**, *31*, 8063.

[74] E. Schönemann, A. Laschewsky, A. Rosenhahn, *Polymers* **2018**, *10*, 639.

[75] M. Kanamala, W. R. Wilson, M. Yang, B. D. Palmer, Z. Wu, *Biomaterials* **2016**, *85*, 152.

[76] L. Nuhn, S. Van Herck, A. Best, K. Deswarte, M. Kokkinopoulou, I. Lieberwirth, K. Koynov, B. N. Lambrecht, B. G. De Geest, *Angewandte Chemie International Edition* **2018**, *57*, 10760.

[77] L. Zhao, L. Shi, J. Wang, Q. Zhang, X. Yang, Y. Lu, *null* **2020**, *69*, 317.

[78] E. M. Bachelder, T. T. Beaudette, K. E. Broaders, J. Dashe, J. M. J. Fréchet, *J. Am. Chem. Soc.* **2008**, *130*, 10494.

[79] E. M. Higbee-Dempsey, A. Amirshaghaghi, M. J. Case, M. Bouché, J. Kim, D. P. Cormode, A. Tsourkas, *J. Am. Chem. Soc.* **2020**, *142*, 7783.

[80] J. C. Love, L. A. Estroff, J. K. Kriebel, R. G. Nuzzo, G. M. Whitesides, *Chem. Rev.* **2005**, *105*, 1103.

[81] C. Vericat, G. A. Benitez, D. E. Grumelli, M. E. Vela, R. C. Salvarezza, *J. Phys.: Condens. Matter* **2008**, *20*, 184004.

[82] Y. Zhang, R. H. Terrill, P. W. Bohn, *Chem. Mater.* **1999**, *11*, 2191.

[83] J. R. Scott, L. S. Baker, W. R. Everett, C. L. Wilkins, I. Fritsch, *Anal. Chem.* **1997**, *69*, 2636.

[84] Y. Li, J. Huang, R. T. McIver, J. C. Hemminger, *J. Am. Chem. Soc.* **1992**, *114*, 2428.

[85] L. Srisombat, A. C. Jamison, T. R. Lee, *Colloids and Surfaces A: Physicochemical and Engineering Aspects* **2011**, *390*, 1.

[86] Y. Joseph, B. Guse, G. Nelles, *Chem. Mater.* **2009**, *21*, 1670.

[87] M. Dasog, R. W. J. Scott, *Langmuir* **2007**, *23*, 3381.

[88] W. Hou, M. Dasog, R. W. J. Scott, *Langmuir* **2009**, *25*, 12954.

[89] N. Bhatt, P.-J. J. Huang, N. Dave, J. Liu, *Langmuir* **2011**, *27*, 6132.

[90] S.-H. Lee, W.-C. Lin, C.-H. Kuo, M. Karakachian, Y.-C. Lin, B.-Y. Yu, J.-J. Shyue, *J. Phys. Chem. C* **2010**, *114*, 10512.

[91] J. Aldana, Y. A. Wang, X. Peng, *J. Am. Chem. Soc.* **2001**, *123*, 8844.

[92] Joshi-BarrShivanjali, de G. LuxCaroline, MahmoudEnas, AlmutairiAdah, *Antioxidants & Redox Signaling* **2014**, DOI 10.1089/ars.2013.5754.

[93] Q. Xu, C. He, C. Xiao, X. Chen, *Macromolecular Bioscience* **2016**, *16*, 635.

[94] F. Scholz, G. López de Lara González, L. Machado de Carvalho, M. Hilgemann, K. Z. Brainina, H. Kahlert, R. S. Jack, D. T. Minh, *Angewandte Chemie International Edition* **2007**, *46*, 8079.

[95] M. Ravandeh, D. Thal, H. Kahlert, K. Wende, M. Lalk, *J Solid State Electrochem* **2020**, *24*, 3003.

[96] J. Duan, D. L. Kasper, *Glycobiology* **2011**, *21*, 401.

[97] R. Cheng, F. Feng, F. Meng, C. Deng, J. Feijen, Z. Zhong, *Journal of Controlled Release* **2011**, *152*, 2.

[98] X. Guo, Y. Cheng, X. Zhao, Y. Luo, J. Chen, W.-E. Yuan, *J Nanobiotechnol* **2018**, *16*, 74.

[99] P. Kuppusamy, H. Li, G. Ilangovan, A. J. Cardounel, J. L. Zweier, K. Yamada, M. C. Krishna, J. B. Mitchell, *Cancer Res* **2002**, *62*, 307.

[100] L. Zhang, K. D. Tew, in *Advances in Cancer Research*, Elsevier, **2021**, pp. 383–413.

[101] L. Brülisauer, M. A. Gauthier, J.-C. Leroux, *Journal of Controlled Release* **2014**, *195*, 147.

[102] M. Chanana, P. Rivera_Gil, M. A. Correa-Duarte, L. M. Liz-Marzán, W. J. Parak, *Angewandte Chemie International Edition* **2013**, *52*, 4179.

[103] D. F. Williams, S. P. Zhong, *International Biodeterioration & Biodegradation* **1994**, *34*, 95.

[104] T. Kean, M. Thanou, *Advanced Drug Delivery Reviews* **2010**, *62*, 3.

[105] O. Franssen, R. D. van Ooijen, D. de Boer, R. A. A. Maes, W. E. Hennink, *Macromolecules* **1999**, *32*, 2896.

[106] O. Lunov, T. Syrovets, C. Röcker, K. Tron, G. Ulrich Nienhaus, V. Rasche, V. Mailänder, K. Landfester, T. Simmet, *Biomaterials* **2010**, *31*, 9015.

[107] K. Herzog, R.-J. Müller, W.-D. Deckwer, *Polymer Degradation and Stability* **2006**, *91*, 2486.

[108] D. M. Yourtee, R. E. Smith, K. A. Russo, S. Burmaster, J. M. Cannon, J. D. Eick, E. L. Kostoryz, *Journal of Biomedical Materials Research* **2001**, *57*, 522.

[109] T. Akagi, M. Higashi, T. Kaneko, T. Kida, M. Akashi, *Biomacromolecules* **2006**, *7*, 297.

[110] K. Bhattacharya, C. Sacchetti, R. El-Sayed, A. Fornara, G. P. Kotchey, J. A. Gaugler, A. Star, M. Bottini, B. Fadeel, *Nanoscale* **2014**, *6*, 14686.

[111] L. Zhu, B. Pelaz, I. Chakraborty, W. J. Parak, *International Journal of Molecular Sciences* **2019**, *20*, 935.

[112] F. B. Landry, D. V. Bazile, G. Spenlehauer, M. Veillard, J. Kreuter, *Biomaterials* **1996**, *17*, 715.

[113] V. Sée, P. Free, Y. Cesbron, P. Nativo, U. Shaheen, D. J. Rigden, D. G. Spiller, D. G. Fernig, M. R. H. White, I. A. Prior, M. Brust, B. Lounis, R. Lévy, *ACS Nano* **2009**, *3*, 2461.

[114] R. Böttger, R. Hoffmann, D. Knappe, *PLOS ONE* **2017**, *12*, e0178943.

[115] D. S. Seferos, A. E. Prigodich, D. A. Giljohann, P. C. Patel, C. A. Mirkin, *Nano Lett.* **2009**, *9*, 308.

[116] Q. Hu, P. S. Katti, Z. Gu, *Nanoscale* **2014**, *6*, 12273.

[117] M. Shahriari, M. Zahiri, K. Abnous, S. M. Taghdisi, M. Ramezani, M. Alibolandi, *Journal of Controlled Release* **2019**, *308*, 172.

[118] S. Alex, A. Tiwari, *Journal of Nanoscience and Nanotechnology* **2015**, *15*, 1869.

[119] S. J. Amina, B. Guo, *Int J Nanomedicine* **2020**, *15*, 9823.

[120] M. J. Hostetler, S. J. Green, J. J. Stokes, R. W. Murray, *J. Am. Chem. Soc.* **1996**, *118*, 4212.

[121] E. C. Dreaden, A. M. Alkilany, X. Huang, C. J. Murphy, M. A. El-Sayed, *Chem. Soc. Rev.* **2012**, *41*, 2740.

[122] J. Turkevich, P. C. Stevenson, J. Hillier, **1951**, DOI 10.1039/DF9511100055.

[123] M. Brust, M. Walker, D. Bethell, D. J. Schiffrin, R. Whyman, *J. Chem. Soc., Chem. Commun.* **1994**, 801.

[124] A. S. D. S. Indrasekara, R. C. Wadams, L. Fabris, *Particle & Particle Systems Characterization* **2014**, *31*, 819.

[125] V. I. Shubayev, T. R. Pisanic, S. Jin, *Advanced Drug Delivery Reviews* **2009**, *61*, 467.

[126] M. Mahmoudi, S. Sant, B. Wang, S. Laurent, T. Sen, *Advanced Drug Delivery Reviews* **2011**, *63*, 24.

[127] K. Davis, B. Cole, M. Ghelardini, B. A. Powell, O. T. Mefford, *Langmuir* **2016**, *32*, 13716.

[128] L. S. Arias, J. P. Pessan, A. P. M. Vieira, T. M. T. de Lima, A. C. B. Delbem, D. R. Monteiro, *Antibiotics (Basel)* **2018**, *7*, E46.

[129] B.-K. Pong, B. L. Trout, J.-Y. Lee, *Langmuir* **2008**, *24*, 5270.

[130] W. Kong, T. Sun, B. Chen, X. Chen, F. Ai, X. Zhu, M. Li, W. Zhang, G. Zhu, F. Wang, *Inorg. Chem.* **2017**, *56*, 872.

[131] R. Hong, G. Han, J. M. Fernández, B. Kim, N. S. Forbes, V. M. Rotello, *J. Am. Chem. Soc.* **2006**, *128*, 1078.

[132] A. Chompoosor, G. Han, V. M. Rotello, *Bioconjugate Chem.* **2008**, *19*, 1342.

[133] T. A. Larson, P. P. Joshi, K. Sokolov, *ACS Nano* **2012**, *6*, 9182.

[134] F. Silva, L. Gano, M. P. C. Campello, R. Marques, I. Prudêncio, A. Zambre, A. Upendran, A. Paulo, R. Kannan, *Dalton Trans.* **2017**, *46*, 14572.

[135] S. Han, T. Zal, K. V. Sokolov, *ACS Nano* **2021**, DOI 10.1021/acsnano.0c08128.

[136] M. Bélanger-Bouliga, R. Mahious, P. Iman Pitroipa, A. Nazemi, *Dalton Transactions* **2021**, *50*, 5598.

[137] J. H. Dunlap, A. F. Loszko, R. A. Flake, Y. Huang, B. C. Benicewicz, A. B. Greytak, *J. Phys. Chem. C* **2018**, *122*, 26756.

[138] R. L. Pinals, D. Yang, A. Lui, W. Cao, M. P. Landry, *J. Am. Chem. Soc.* **2020**, *142*, 1254.

[139] G. Ruiz, N. Ryan, K. Rutschke, O. Awotunde, J. D. Driskell, *Langmuir* **2019**, *35*, 10601.

[140] X. Wang, X. Wang, X. Bai, L. Yan, T. Liu, M. Wang, Y. Song, G. Hu, Z. Gu, Q. Miao, C. Chen, *Nano Lett.* **2019**, *19*, 8.

[141] G. Chong, I. U. Foreman-Ortiz, M. Wu, A. Bautista, C. J. Murphy, J. A. Pedersen, R. Hernandez, *J. Phys. Chem. C* **2019**, *123*, 27951.

[142] Y. Song, R. W. Murray, *J. Am. Chem. Soc.* **2002**, *124*, 7096.

[143] M. Montalti, L. Prodi, N. Zaccheroni, R. Baxter, G. Teobaldi, F. Zerbetto, *Langmuir* **2003**, *19*, 5172.

[144] C. L. Heinecke, T. W. Ni, S. Malola, V. Mäkinen, O. A. Wong, H. Häkkinen, C. J. Ackerson, *J. Am. Chem. Soc.* **2012**, *134*, 13316.

[145] P. Ionita, A. Caragheorgheopol, B. C. Gilbert, V. Chechik, *J. Am. Chem. Soc.* **2002**, *124*, 9048.

[146] P. Ionita, A. Caragheorgheopol, B. C. Gilbert, V. Chechik, *Langmuir* **2004**, *20*, 11536.

[147] M. Zachary, V. Chechik, *Angewandte Chemie International Edition* **2007**, *46*, 3304.

[148] Y. Song, T. Huang, R. W. Murray, *J. Am. Chem. Soc.* **2003**, *125*, 11694.

[149] E. Villarreal, G. G. Li, Q. Zhang, X. Fu, H. Wang, *Nano Lett.* **2017**, *17*, 4443.

[150] A. Fernando, C. M. Aikens, *J. Phys. Chem. C* **2015**, *119*, 20179.

[151] R. Dinkel, B. Braunschweig, W. Peukert, *J. Phys. Chem. C* **2016**, *120*, 1673.

[152] S. Zhang, S. Kim, V. V. Tsukruk, *Langmuir* **2017**, *33*, 3576.

[153] M. Kluenker, M. Mondeshki, M. Nawaz Tahir, W. Tremel, *Langmuir* **2018**, *34*, 1700.

[154] S. Athukorale, M. De Silva, A. LaCour, G. S. Perera, C. U. Pittman, D. Zhang, *J. Phys. Chem. C* **2018**, *122*, 2137.

[155] R. Dinkel, J. Jakobi, A. R. Ziefuß, S. Barcikowski, B. Braunschweig, W. Peukert, *J. Phys. Chem. C* **2018**, *122*, 27383.

[156] Z. Luo, J. Hou, L. Menin, Q. K. Ong, F. Stellacci, *Angewandte Chemie* **2017**, *129*, 13706.

[157] A. Lapresta-Fernández, E. Nefeli Athanasopoulou, P. Jacob Silva, Z. Pelin Güven, F. Stellacci, *Journal of Colloid and Interface Science* **2022**, *616*, 110.

[158] O. Awotunde, S. Okyem, R. Chikoti, J. D. Driskell, *Langmuir* **2020**, *36*, 9241.

[159] K. Davis, M. Vidmar, A. Khasanov, B. Cole, M. Ghelardini, J. Mayer, C. Kitchens, A. Nath, B. A. Powell, O. T. Mefford, *Journal of Colloid and Interface Science* **2018**, *511*, 374.

[160] J. J. Calvin, E. A. O'Brien, A. B. Sedlak, A. D. Balan, A. P. Alivisatos, *ACS Nano* **2021**, *15*, 1407.

[161] A. M. Smith, L. E. Marbella, K. A. Johnston, M. J. Hartmann, S. E. Crawford, L. M. Kozycz, D. S. Seferos, J. E. Millstone, *Anal. Chem.* **2015**, *87*, 2771.

[162] H.-M. Gao, H. Liu, H.-J. Qian, G.-S. Jiao, Z.-Y. Lu, *Physical Chemistry Chemical Physics* **2018**, *20*, 1381.

[163] M. Liu, Y.-Y. Wang, Y. Liu, F.-L. Jiang, *J. Phys. Chem. C* **2020**, *124*, 4613.

[164] H. Wei, W. Leng, J. Song, C. Liu, M. R. Willner, Q. Huang, W. Zhou, P. J. Vikesland, *Environ. Sci. Technol.* **2019**, *53*, 575.

[165] B. C. Mei, E. Oh, K. Susumu, D. Farrell, T. J. Mountziaris, H. Mattoussi, *Langmuir* **2009**, *25*, 10604.

[166] F. Schulz, T. Vossmeyer, N. G. Bastús, H. Weller, *Langmuir* **2013**, *29*, 9897.

[167] F. Li, H. Zhang, B. Dever, X.-F. Li, X. C. Le, *Bioconjugate Chem.* **2013**, *24*, 1790.

[168] R. Hong, J. M. Fernández, H. Nakade, R. Arvizo, T. Emrick, V. M. Rotello, *Chem. Commun.* **2006**, 2347.

[169] C. Goldmann, F. Ribot, L. F. Peiretti, P. Quaino, F. Tielens, C. Sanchez, C. Chanéac, D. Portehault, *Small* **2017**, *13*, 1604028.

[170] R. Guo, Y. Song, G. Wang, R. W. Murray, *J. Am. Chem. Soc.* **2005**, *127*, 2752.

[171] C.-H. Chan, F. Poignant, M. Beuve, E. Dumont, D. Loffreda, *J. Phys. Chem. Lett.* **2020**, *11*, 2717.

[172] N. Yan, N. Xia, Z. Wu, *Small* **2020**, 2000609.

[173] Z. Qing, G. Luo, S. Xing, Z. Zou, Y. Lei, J. Liu, R. Yang, *Angewandte Chemie International Edition* **2020**, *59*, 14044.

[174] K. Rana, J. R. Bhamore, J. V. Rohit, T.-J. Park, S. Kumar Kailasa, *New Journal of Chemistry* **2018**, *42*, 9080.

[175] A. Lesiak, K. Halicka, M. Chrzanowski, M. Banski, A. Żak, J. Cabaj, A. Podhorodecki, *J Nanopart Res* **2020**, *22*, 238.

[176] W. Wei, X. Zhang, S. Zhang, G. Wei, Z. Su, *Materials Science and Engineering: C* **2019**, *104*, 109891.

[177] C. J. Chen, R. M. Osgood, *Phys. Rev. Lett.* **1983**, *50*, 1705.

[178] K. Ueno, H. Misawa, *Journal of Photochemistry and Photobiology C: Photochemistry Reviews* **2013**, *15*, 31.

[179] Z. Zhang, P. Xu, X. Yang, W. Liang, M. Sun, *Journal of Photochemistry and Photobiology C: Photochemistry Reviews* **2016**, *27*, 100.

[180] C. Zhan, X.-J. Chen, J. Yi, J.-F. Li, D.-Y. Wu, Z.-Q. Tian, *Nat Rev Chem* **2018**, *2*, 216.

[181] H.-H. Shin, J.-J. Koo, K. S. Lee, Z. H. Kim, *Applied Materials Today* **2019**, *16*, 112.

[182] C. Zhang, F. Jia, Z. Li, X. Huang, G. Lu, *Nano Res.* **2020**, *13*, 3183.

[183] I. Kherbouche, Y. Luo, N. Félidj, C. Mangeney, *Chem. Mater.* **2020**, *32*, 5442.

[184] M. Sun, H. Xu, *Small* **2012**, *8*, 2777.

[185] J. L. Brooks, R. R. Frontiera, *J. Phys. Chem. C* **2016**, *120*, 20869.

[186] B. Kafle, M. Poveda, T. G. Habteyes, *J. Phys. Chem. Lett.* **2017**, *8*, 890.

[187] H. Kookhaee, T. E. Tesema, T. G. Habteyes, *J. Phys. Chem. C* **2020**, *124*, 22711.

[188] H. Wei, S. K. Loeb, N. J. Halas, J.-H. Kim, *PNAS* **2020**, *117*, 15473.

[189] R. Huschka, J. Zuloaga, M. W. Knight, L. V. Brown, P. Nordlander, N. J. Halas, *J. Am. Chem. Soc.* **2011**, *133*, 12247.

[190] K. Metwally, S. Mensah, G. Baffou, *J. Phys. Chem. C* **2015**, *119*, 28586.

[191] P. Kang, Z. Chen, S. O. Nielsen, K. Hoyt, S. D'Arcy, J. J. Gassensmith, Z. Qin, *Small* **2017**, *13*, 1700841.

[192] A. Carattino, M. Caldarola, M. Orrit, *Nano Lett.* **2018**, *18*, 874.

[193] D. A. Hastman, P. Chaturvedi, E. Oh, J. S. Melinger, I. L. Medintz, L. Vuković, S. A. Díaz, *ACS Appl. Mater. Interfaces* **2022**, *14*, 3404.

[194] J. R. Lepock, Harold E. Frey, Kenneth P. Ritchi, *J Cell Biol* **1993**, *122*, 1267.

[195] Z.-C. Zeng, H. Wang, P. Johns, G. V. Hartland, Z. D. Schultz, *J. Phys. Chem. C* **2017**, *121*, 11623.

[196] M. You, P. Jia, X. He, Z. Wang, S. Feng, Y. Ren, Z. Li, L. Cao, B. Gao, C. Yao, S. Singamaneni, F. Xu, *Small Methods* **2021**, *5*, 2001254.

[197] A. B. S. Bakhtiari, D. Hsiao, G. Jin, B. D. Gates, N. R. Branda, *Angewandte Chemie* **2009**, *121*, 4230.

[198] S. Yamashita, H. Fukushima, Y. Niidome, T. Mori, Y. Katayama, T. Niidome, *Langmuir* **2011**, *27*, 14621.

[199] K. Bolaños, M. Sánchez-Navarro, E. Giralt, G. Acosta, F. Albericio, M. J. Kogan, E. Araya, *Materials Science and Engineering: C* **2021**, *131*, 112512.

[200] J. Huang, K. S. Jackson, C. J. Murphy, *Nano Lett.* **2012**, *12*, 2982.

[201] W. Lin, C. J. Murphy, *ACS Cent. Sci.* **2017**, *3*, 1096.

[202] M. Mahmoudi, S. E. Lohse, C. J. Murphy, A. Fathizadeh, A. Montazeri, K. S. Suslick, *Nano Lett.* **2014**, *14*, 6.

[203] M. Javad Hajipour, O. Akhavan, A. Meidanchi, S. Laurent, M. Mahmoudi, *RSC Advances* **2014**, *4*, 62557.

[204] F. Hashemi, M. Reza Hormozi-Nezhad, C. Corbo, F. Farvadi, M. Ali Shokrgozar, M. Mehrjoo, F. Atyabi, M. Hossein Ghahremani, M. Mahmoudi, R. Dinarvand, *Nanoscale* **2019**, *11*, 5974.

[205] E. Polo, V. Araban, B. Pelaz, A. Alvarez, P. Taboada, M. Mahmoudi, P. del Pino, *Applied Materials Today* **2019**, *15*, 599.

[206] K. Bolaños, F. Celis, C. Garrido, M. Campos, F. Guzmán, M. J Kogan, E. Araya, *Journal of Materials Chemistry B* **2020**, *8*, 8644.

[207] X. Cheng, T. P. Anthony, C. A. West, Z. Hu, V. Sundaresan, A. J. McLeod, D. J. Masiello, K. A. Willets, *J. Phys. Chem. Lett.* **2019**, *10*, 1394.

[208] G. Baffou, H. Rigneault, *Phys. Rev. B* **2011**, *84*, 035415.

[209] P. K. Jain, W. Qian, M. A. El-Sayed, *J. Am. Chem. Soc.* **2006**, *128*, 2426.

[210] L. Poon, W. Zandberg, D. Hsiao, Z. Erno, D. Sen, B. D. Gates, N. R. Branda, *ACS Nano* **2010**, *4*, 6395.

[211] F. Thibaudau, *J. Phys. Chem. Lett.* **2012**, *3*, 902.

[212] D. A. Hastman, J. S. Melinger, G. L. Aragonés, P. D. Cunningham, M. Chiriboga, Z. J. Salvato, T. M. Salvato, C. W. Brown, D. Mathur, I. L. Medintz, E. Oh, S. A. Díaz, *ACS Nano* **2020**, *14*, 8570.

[213] A. M. Goodman, N. J. Hogan, S. Gottheim, C. Li, S. E. Clare, N. J. Halas, *ACS Nano* **2017**, *11*, 171.

[214] C. Jack, A. S. Karimullah, R. Tullius, L. K. Khorashad, M. Rodier, B. Fitzpatrick, L. D. Barron, N. Gadegaard, A. J. Lapthorn, V. M. Rotello, G. Cooke, A. O. Govorov, M. Kadodwala, *Nat Commun* **2016**, *7*, 10946.

[215] A. Dabbagh, Z. Hedayatnasab, H. Karimian, M. Sarraf, C. H. Yeong, H. R. Madaah Hosseini, N. H. Abu Kasim, T. W. Wong, N. A. Rahman, *International Journal of Hyperthermia* **2019**, *36*, 104.

[216] M. Le Goas, A. Paquirissamy, D. Gargouri, G. Fadda, F. Testard, C. Aymes-Chodur, E. Jubeli, T. Pourcher, B. Cambien, S. Palacin, J.-P. Renault, G. Carrot, *ACS Appl. Bio Mater.* **2019**, *2*, 144.

[217] B. Yan, Y. Jeong, L. A. Mercante, G. Y. Tonga, C. Kim, Z.-J. Zhu, R. W. Vachet, V. M. Rotello, *Nanoscale* **2013**, *5*, 5063.

[218] J. H. O'Donnell, in *Radiation Effects on Polymers*, American Chemical Society, **1991**, pp. 402–413.

[219] K. Heister, M. Zharnikov, M. Grunze, L. S. O. Johansson, A. Ulman, *Langmuir* **2001**, *17*, 8.

[220] M. A. Vetten, C. S. Yah, T. Singh, M. Gulumian, *Nanomedicine: Nanotechnology, Biology and Medicine* **2014**, *10*, 1391.

[221] Z. Kuncic, S. Lacombe, *Phys. Med. Biol.* **2018**, *63*, 02TR01.

[222] I. Kempson, *WIREs Nanomedicine and Nanobiotechnology* **2021**, *13*, e1656.

[223] A. V. Verkhovtsev, A. V. Korol, A. V. Solov'yov, *Phys. Rev. Lett.* **2015**, *114*, 063401.

[224] Z. B. Starkewolf, L. Miyachi, J. Wong, T. Guo, *Chemical Communications* **2013**, *49*, 2545.

[225] C. van Ballegooie, A. Man, A. Pallaoro, M. Bally, B. D. Gates, D. T. Yapp, *Pharmaceutics* **2021**, *13*, 1407.

[226] G. Gaur, D. S. Koktysh, D. M. Fleetwood, R. A. Weller, R. A. Reed, B. R. Rogers, S. M. Weiss, *ACS Appl. Mater. Interfaces* **2016**, *8*, 7869.

[227] F. Xiao, Y. Zheng, P. Cloutier, Y. He, D. Hunting, L. Sanche, *Nanotechnology* **2011**, *22*, 465101.

[228] K. Haume, P. de Vera, A. Verkhovtsev, E. Surdutovich, N. J. Mason, A. V. Solov'yov, *European Physical Journal D* **2018**, *72*.

[229] F. Hespeels, A.-C. Heuskin, T. Tabarrant, E. Scifoni, M. Kraemer, G. Chêne, D. Strivay, S. Lucas, *Phys. Med. Biol.* **2019**, DOI 10.1088/1361-6560/ab195f.

[230] M. Gilles, E. Brun, C. Sicard-Roselli, *Colloids and Surfaces B: Biointerfaces* **2014**, *123*, 770.

[231] C. Spaas, R. Dok, O. Deschaume, B. De Roo, M. Vervaele, J. W. Seo, C. Bartic, P. Hoet, F. Van den Heuvel, S. Nuyts, J.-P. Locquet, *Radiation Research* **2016**, *185*, 384.

[232] D. Peukert, I. Kempson, M. Douglass, E. Bezak, *Medical Physics* **2020**, *47*, 651.

[233] R. Borah, R. Ninakanti, G. Nuyts, H. Peeters, A. Pedrazo-Tardajos, S. Nuti, C. V. Velde, K. D. Wael, S. Lenaerts, S. Bals, S. W. Verbruggen, *Chemistry – A European Journal* **2021**, *27*, 9011.

[234] B. Yan, Z.-J. Zhu, O. R. Miranda, A. Chompoosor, V. M. Rotello, R. W. Vachet, *Anal Bioanal Chem* **2010**, *396*, 1025.

[235] Y. Chen, Z. Wang, Y. He, Y. J. Yoon, J. Jung, G. Zhang, Z. Lin, *PNAS* **2018**, *115*, E1391.

[236] B. Kokot, H. Kokot, P. Umek, K. P. van Midden, S. Pajk, M. Garvas, C. Eggeling, T. Koklič, I. Urbančič, J. Štrancar, *Nanotoxicology* **2021**, *15*, 1102.

[237] A. M. Milosevic, L. Haeni, L. Ackermann Hirschi, S. Vanni, P. Campomanes-Ramos, B. Rothen-Rutishauser, L. Rodriguez-Lorenzo, A. Petri-Fink, *ChemNanoMat* **2022**, *8*, e202100443.

[238] D. Bargheer, J. Nielsen, G. Gébel, M. Heine, S. C. Salmen, R. Stauber, H. Weller, J. Heeren, P. Nielsen, *Beilstein Journal of Nanotechnology* **2015**, *6*, 36.

[239] H. Wang, R. Kumar, D. Nagesha, R. I. Duclos, S. Sridhar, S. J. Gatley, *Nuclear Medicine and Biology* **2015**, *42*, 65.

[240] T. Chen, B. He, J. Tao, Y. He, H. Deng, X. Wang, Y. Zheng, *Advanced Drug Delivery Reviews* **2019**, *143*, 177.

[241] Z.-J. Zhu, Y.-C. Yeh, R. Tang, B. Yan, J. Tamayo, R. W. Vachet, V. M. Rotello, *Nature Chem* **2011**, *3*, 963.

[242] Z.-J. Zhu, R. Tang, Y.-C. Yeh, O. R. Miranda, V. M. Rotello, R. W. Vachet, *Anal. Chem.* **2012**, *84*, 4321.

[243] Y. Portilla, S. Mellid, A. Paradela, A. Ramos-Fernández, N. Daviu, L. Sanz-Ortega, S. Pérez-Yagüe, M. P. Morales, D. F. Barber, *ACS Appl. Mater. Interfaces* **2021**, *13*, 7924.

[244] S. J. H. Soenen, U. Himmelreich, N. Nuytten, T. R. Pisanic, A. Ferrari, M. De Cuyper, *Small* **2010**, *6*, 2136.

[245] Z. Liu, A. Escudero, C. Carrillo-Carrion, I. Chakraborty, D. Zhu, M. Gallego, W. J. Parak, N. Feliu, *Chem. Mater.* **2020**, *32*, 245.

[246] H. Chen, P. Zou, J. Connarn, H. Paholak, D. Sun, *Nano Res.* **2012**, *5*, 815.

[247] C. Carrillo-Carrion, A. I. Bocanegra, B. Arnaiz, N. Feliu, D. Zhu, W. J. Parak, *ACS Nano* **2019**, *13*, 4631.

[248] N. L. Rosi, D. A. Giljohann, C. S. Thaxton, A. K. R. Lytton-Jean, M. S. Han, C. A. Mirkin, *Science* **2006**, *312*, 1027.

[249] L. Shang, L. Yang, H. Wang, G. U. Nienhaus, *Small* **2016**, *12*, 868.

[250] S. Sindhwani, A. M. Syed, J. Ngai, B. R. Kingston, L. Maiorino, J. Rothschild, P. MacMillan, Y. Zhang, N. U. Rajesh, T. Hoang, J. L. Y. Wu, S. Wilhelm, A. Zilman, S. Gadde, A. Sulaiman, B. Ouyang, Z. Lin, L. Wang, M. Egeblad, W. C. W. Chan, *Nature Materials* **2020**, *19*, 566.

[251] P. Bourrinet, H. H. Bengele, B. Bonnemain, A. Dencausse, J.-M. Idee, P. M. Jacobs, J. M. Lewis, *Invest Radiol* **2006**, *41*, 313.

[252] R. Tietze, C. Alexiou, *Nanomedicine* **2017**, *12*, 167.

[253] X. Li, H. Yu, B. Wang, W. Chen, M. Zhu, S. Liang, R. Chu, S. Zhou, H. Chen, M. Wang, L. Zheng, W. Feng, *ACS Biomater. Sci. Eng.* **2021**, *7*, 1462.

[254] H. Y. Yang, Y. Fu, M.-S. Jang, Y. Li, J. H. Lee, H. Chae, D. S. Lee, *ACS Appl. Mater. Interfaces* **2016**, *8*, 35021.

[255] Y. Xue, X. Li, H. Li, W. Zhang, *Nat Commun* **2014**, *5*, 4348.

[256] W. Wei, Y. Sun, M. Zhu, X. Liu, P. Sun, F. Wang, Q. Gui, W. Meng, Y. Cao, J. Zhao, *J. Am. Chem. Soc.* **2015**, *137*, 15358.

[257] A. Giorgio, A. Merlino, *Coordination Chemistry Reviews* **2020**, *407*, 213175.

[258] L. A. Low, C. Mummery, B. R. Berridge, C. P. Austin, D. A. Tagle, *Nat Rev Drug Discov* **2021**, *20*, 345.

[259] S. Hua, M. B. C. de Matos, J. M. Metselaar, G. Storm, *Frontiers in Pharmacology* **2018**, *9*, DOI 10.3389/fphar.2018.00790.

[260] J.-M. Rabanel, V. Adibnia, S. F. Tehrani, S. Sanche, P. Hildgen, X. Banquy, C. Ramassamy, *Nanoscale* **2019**, *11*, 383.

[261] H. Zhao, H. Meng, Q. Zhang, Y. Wu, H. Chen, X. Jiang, C. Zhang, *Environ. Sci.: Nano* **2022**, *9*, 313.

[262] L. Wang, P. Quan, S. H. Chen, W. Bu, Y.-F. Li, X. Wu, J. Wu, L. Zhang, Y. Zhao, X. Jiang, B. Lin, R. Zhou, C. Chen, *ACS Nano* **2019**, *13*, 8680.

[263] F. Peng, M. I. Setyawati, J. K. Tee, X. Ding, J. Wang, M. E. Nga, H. K. Ho, D. T. Leong, *Nature Nanotechnology* **2019**, *14*, 279.